

INVESTIGATING THE IMPACT OF RESIDENTIAL SOLAR PV SYSTEM INTEGRATION ON POWER QUALITY IN A DISTRIBUTION NETWORK



Prepared by:
Crystal Jaftha
JFTCRY001

Department of Electrical Engineering
University of Cape Town

Prepared for:
Sunetra Chowdhury

Department of Electrical Engineering
University of Cape Town

6 November 2022

Submitted to the Department of Electrical Engineering at the University of Cape Town in partial fulfilment
of the academic requirements for a Bachelor of Science degree in Mechatronics Engineering

Key Words: Solar photovoltaic (PV) Plant, Power Quality, Distribution Network

Plagiarism Declaration

1. I know that plagiarism is wrong. Plagiarism is to use another's work and pretend that it is one's own.
2. I have used the IEEE convention for citation and referencing. Each contribution to, and quotation in, this final year project report from the work(s) of other people, has been attributed and has been cited and referenced.
3. This final year project report is my own work.
4. I have not allowed, and will not allow, anyone to copy my work with the intention of passing it off as their own work or part thereof

Name:

Crystal Jaftha

Signature:



Date: 06 November 2022

Terms of Reference

The undergraduate thesis topic of “Investigating the impact of residential solar PV system integration on power quality in a distribution network” was proposed by A/Prof. S. Chowdhury. The project was conducted throughout the second academic semester of 2022. The deliverables of the project are as follows:

- Review of power quality challenges in a distribution network.
- Review of the impact of residential solar PV system integration on power quality.
- Design a distribution network with solar PV systems integrated into it where the design steps followed are shown.
- Develop criteria for investigating the power quality deviation and identify the points of PV integration in the network where this deviation could be minimized.
- Interpret results and conclusions and suggest recommendations.

Acknowledgements

I would like to express my sincere gratitude to the following individuals for their assistance in completing my research project:

My supervisor, A/Prof. S. Chowdhury, who has assisted me throughout the semester and guided me onto the right path to success.

My parents who have made many sacrifices for my benefit and have given me the opportunity to study at UCT. I am thankful for their endless support and encouragement.

My classmates, Azhar, Salmaan, and Raees, who have accompanied and helped me throughout my studies. We all share many fond memories together over the last few years.

My friend, Suvitha, for her daily motivation and support throughout the year.

Abstract

The impact of residential solar PV system integration on power quality in a distribution network is investigated in this report. When small-scale residential solar PV systems are integrated into a distribution grid, the capacity of the plant and its fluctuating generation are likely to impact the power quality of the network in terms of voltage and frequency. In this project, DIgSILENT PowerFactory was used to design distribution networks with the integration of solar PV plants. The project considered different loadings on the distribution feeders and high, medium, and low levels of penetration of solar PV systems in that area. To study the power quality of the system, voltage and frequency profiles for the distribution networks were simulated and analysed against a base case, which did not include the integration of PV plants. The voltage and frequency deviations were calculated and the magnitudes of the simulated voltages and frequencies complied with standard South African grid codes for renewable energy integration. It was discovered that power quality is impacted by various factors in a distribution network such as distribution voltage levels, penetration levels, and load variation.

Nomenclature

RES: Renewable Energy System
PV: Photovoltaic Cell
FF: Fill Factor
DG: Distributed Generation
POI: Point of Interface
POC: Point of Connection
LV: Low-Voltage
THD: Total Harmonic Distortion
APC: Active Power Curtailment
EV: Electric Vehicle
PCC: Point of Common Coupling
MPPT: Maximum Power Point Tracking
LMS: Least Mean Square
NLMS: Normalized LMS
IEEE: Institute of Electrical and Electronics Engineers
WECC: Western Electricity Coordinating Council
HV: High Voltage
REMV: Renewable Energy Model Validation

Table of Contents

<i>Plagiarism Declaration</i>	i
<i>Terms of Reference</i>	ii
<i>Acknowledgements</i>	iii
<i>Abstract</i>	iv
<i>Nomenclature</i>	v
<i>List of Figures</i>	ix
<i>List of Tables</i>	x
1. Introduction	1
1.1. Background	1
1.2. Motivation	1
1.3. Problem statement	1
1.4. Objectives	2
1.5. Thesis contributions	2
1.6. Scope and limitations	2
1.7. Thesis outline	2
2. Literature Review	4
2.1. Introduction	4
2.2. Renewable Energy	5
2.3. Introduction to Solar Photovoltaic Cells	5
2.4. Single PV Cell Module Theory	5
2.5. Types of PV Cells	6
2.5.1. Monocrystalline Silicon Cells	6
2.5.2. Polycrystalline Silicon Cells	6
2.5.3. Thin Film Solar Cells	7
2.5.4. Comparison of PV Cells	7
2.6. Benefits of PV Cells	7
2.7. General Applications of PV Cells	7
2.8. Applications of PV Cells in Africa and Other Countries	7
2.8.1. Africa	7
2.8.2. Other Countries	8
2.9. Integration of PV Systems in Distribution Networks	8
2.10. Grid Strength	8
2.11. Renewable Energy Grid Codes in South Africa	8
2.12. Challenges Experienced by PV Plants	9
2.12.1. Fluctuations in Solar Radiation Availability	9
2.12.2. High Penetration Levels in LV Distribution Networks	9
2.12.3. Lightning Strike Phone	9
2.13. Impact of Residential Solar PV System Integration on Power Quality	9
2.13.1. Overvoltage	10
2.13.2. Voltage Fluctuations	10
2.13.3. Poor Power Factor	10
2.13.4. Total Harmonic Distortion	10
2.14. Power Quality Challenge Mitigation Techniques	10
2.14.1. Overvoltage Mitigation Techniques	10
2.14.2. Voltage Fluctuation Mitigation Techniques	11
2.14.3. Poor Power Factor Mitigation Techniques	11
2.14.4. Total Harmonic Distortion Mitigation Techniques	11

2.15. Conclusion	12
3. Methodology	13
3.1. Introduction	13
3.2. Design Overview	13
3.3. Simulation Software Selection	13
3.4. Component Modelling in DIgSILENT	14
3.4.1. IEEE 9-bus Benchmark System	14
3.4.2. Busbars	15
3.4.3. Two-winding Transformers	15
3.4.4. WECC Large-Scale PV Plant 110MVA 60Hz	16
3.4.5. General Loads	17
3.4.6. External Grid	17
3.5. Final Design of the Test System	18
3.6. Simulation of Voltage and Frequency Profiles	18
3.6.1. Three-phase Fault	19
3.6.2. Load Flow Calculation	19
3.7. Planning of Case Studies	19
3.7.1. Case study 1 (Base): Testing of the system with a medium load (75MW) and without the integration of PV plants	19
3.7.2. Case study 2: Testing of the system with low loads (50MW) and with the integration of PV plants	19
3.7.3. Case study 3: Testing of the system with medium loads (75MW) and with the integration of PV plants	19
3.7.4. Case study 4: Testing of the system with high loads (100MW) and with the integration of PV plants	19
4. Results and Discussion	20
4.1. Case Study 1 (Base): Voltage and frequency simulations of the system with medium loads (75MW) and without the integration of Solar PV plants (no penetration)	20
4.1.1. Voltage Profile	20
4.1.2. Frequency Profile	21
4.2. Case Study 2: Voltage and frequency simulations of the system with low loads (50MW) and with varying levels of penetration	22
4.2.1. Low Penetration Levels	22
4.2.2. Medium Penetration Levels	24
4.2.3. High Penetration Levels	26
4.3. Case Study 3: Voltage and frequency simulations of the system with medium loads (75MW) and with varying levels of penetration	28
4.3.1. Low Penetration Levels	28
4.3.2. Medium Penetration Levels	30
4.3.3. High Penetration Levels	32
4.4. Case study 4: Voltage and frequency simulations of the system with high loads (100MW) and with varying levels of penetration	34
4.4.1. Low Penetration Levels	34
4.4.2. Medium Penetration Levels	36
4.4.3. High Penetration Levels	38
4.5. Summary of the Calculated Voltage and Frequency Deviations	40
4.6. Discussion of Results	43
5. Conclusion	44
5.1. Conclusions	44

5.2. Recommendations for Future work	44
5.2.1. Consideration of Other Types of DG Systems	44
5.2.2. Variation of Grid Strength	44
5.2.3. Different Short Circuit Events	44
5.2.4. Consideration of Multiple Points of Integration	44
List of References	45
Appendices	48
<i>Appendix A: System Report and Penetration Levels Percentage Calculations</i>	<i>48</i>
<i>Appendix B: Voltage and Frequency Deviation Calculations on Excel</i>	<i>49</i>
EBE Faculty: Assessment of Ethics in Research Projects	50

List of Figures

Figure 2-1: Diode-connected PV cell equivalent circuit [1]	5
Figure 2-2: Residential PV system connected to the grid [2]	8
Figure 3-1: IEEE 9-bus benchmark system	14
Figure 3-2: WECC Large-Scale PV Plant 110MVA 60Hz modelled in DigSILENT	16
Figure 3-3: IEEE 9-bus system with distribution networks and PV plant integration	18
Figure 4-1: Voltage profile for the base case	20
Figure 4-2: Frequency profile for the base case	21
Figure 4-3: Voltage profile for Case 2 with low penetration levels	22
Figure 4-4: Frequency profile for Case 2 with low penetration levels	23
Figure 4-5: Voltage profile for Case 2 with medium penetration levels	24
Figure 4-6: Frequency profile for Case 2 with medium penetration levels	25
Figure 4-7: Voltage profile for Case 2 with high penetration levels	26
Figure 4-8: Frequency profile for Case 2 with high penetration levels	27
Figure 4-9: Voltage profile for Case 3 with low penetration levels	28
Figure 4-10: Frequency profile for Case 3 with low penetration levels	29
Figure 4-11: Voltage profile for Case 3 with medium penetration levels	30
Figure 4-12: Frequency profile for Case 3 with medium penetration levels	31
Figure 4-13: Voltage profile for Case 3 with high penetration levels	32
Figure 4-14: Frequency profile for Case 3 with high penetration levels	33
Figure 4-15: Voltage profile for Case 4 with low penetration levels	34
Figure 4-16: Frequency profile for Case 4 with low penetration levels	35
Figure 4-17: Voltage profile for Case 4 with medium penetration levels	36
Figure 4-18: Frequency profile for Case 4 with medium penetration levels	37
Figure 4-19: Voltage profile for Case 4 with high penetration levels	38
Figure 4-20: Frequency profile for Case 4 with high penetration levels	39
Figure A-1: Complete system report	48
Figure B-1: Voltage and frequency deviation calculations on Excel	49

List of Tables

Table 2-1: Summary of the topics covered in the literature review	4
Table 2-2: Comparison of the characteristics of each type of PV cell according to efficiency, performance, lifespan, and cost [3][4]	7
Table 2-3: Minimum (U_{\min}) and maximum (U_{\max}) voltages for the POCs of DG systems [5]	9
Table 3-1: Steps describing the methodology	13
Table 3-2: List of components used to construct the test system and their quantities	14
Table 3-3: Line-to-line voltages of the busbars	15
Table 3-4: Parameter configuration for Transformer_1 and Transformer_2	16
Table 3-5: Table specifying the active power values of the PV plant models	17
Table 3-6: Voltages of the transformers for PV_Plant_1 and PV_Plant_2	17
Table 3-7: Table specifying the load values chosen to represent low, medium, and high loads	17
Table 3-8: Parameter configuration of the external grid	18
Table 4-1: Summary of the voltage magnitudes and deviations for Case 2	40
Table 4-2: Summary of the frequency magnitudes and deviations for Case 2	41
Table 4-3: Summary of the voltage magnitudes and deviations for Case 3	41
Table 4-4: Summary of the frequency magnitudes and deviations for Case 3	42
Table 4-5: Summary of the voltage magnitudes and deviations for Case 4	42
Table 4-6: Summary of the frequency magnitudes and deviations for Case 4	43

1. Introduction

1.1. Background

Electricity is a vital aspect of the modern world and is needed for household appliances, electronics, transportation, machinery, etc. Many countries, particularly those in Africa, have limited access to electricity and in countries such as South Africa, load-shedding is an ongoing problem. It is crucial that an affordable and efficient solution to the electricity crisis is found.

In addition to the lack of access to electricity, global warming, the depletion of fossil fuels, population increase, and the increasing cost of fuel are all factors that have prompted more research and the growth of renewable energy systems (RES). RES are desirable as they are sustainable, do not release any toxic emissions, thereby do not cause any harm to humans, animals, or the environment, and they will never deplete. They are therefore considered a suitable solution to help combat the electricity crisis. The most popular RES include hydroelectric power, wind energy, geothermal energy, biomass, and solar power.

Solar power is achieved through the conversion of solar irradiation into electricity through the use of solar photovoltaic (PV) cells. The solar energy industry is becoming popular in numerous countries as solar power has low production costs and is affordable for consumers [6].

Although PV systems can be considered to be an appropriate solution to the high energy demand due to their many advantages, new challenges are introduced when they are integrated into a distribution network to provide electricity for residential use. The output of solar PV systems varies according to the variation in solar resource availability. When small-scale residential solar PV systems are integrated into a distribution grid without proper planning, the capacity of the plant and its fluctuating generation have an impact on the voltage and frequency components of power quality of the network leading to power quality problems. This project focuses on investigating the impact of residential solar photovoltaic system integration on power quality in a distribution network.

1.2. Motivation

The goal of this project is to demonstrate how power quality is affected by the integration of PV systems in a distribution network. It is important to investigate how the power quality is affected in order to find ways to reduce these effects and mitigate the problems to achieve optimal power quality. PV system integration in distribution grids can be improved globally and power quality can be optimized. Optimal power quality is crucial for the high efficiency of power systems, reducing the cost of energy production and preventing equipment damage.

Additionally, this project is motivated by the global need for clean, efficient, and affordable RES. By mitigating the challenges associated with PV systems, the integration of solar PV systems in distribution networks can become the best practice for providing energy to residential areas.

1.3. Problem Statement

The output of solar PV systems varies according to the variation in solar resource availability. When small-scale residential solar PV systems are integrated into a distribution grid, the capacity of the plant and its fluctuating generation are likely to impact the voltage and frequency components of the power quality of the network.

1.4. Objectives

The primary objective of this thesis is to investigate the impact of residential solar PV system integration on power quality in a distribution network, by using software programs to simulate the systems and analyse their behaviour.

The specific sub-objectives of the thesis are as follows:

- Review of power quality challenges in a distribution network.
- Review of the impact of residential solar PV system integration on power quality.
- Design a distribution network with solar PV systems integrated into it where the design steps followed are shown.
- Develop a criterion for investigating the power quality deviation and identify the points of PV integration in the network where this deviation could be minimized.
- Interpret results and conclusions and suggest recommendations.

1.5. Thesis Contributions

The main contributions of this thesis were to design and simulate a distribution network with a solar PV system integrated using a power systems simulation software to it to investigate the power quality deviation and identify the points in the network where this deviation will be measured.

1.6. Scope and Limitations

The scope of the thesis is to design a residential distribution network with solar PV systems integrated into it to observe how power quality is affected. The power quality issues that were reviewed include overvoltage, voltage fluctuations, poor power factor, and total harmonic distortion. The project did not include the consideration of other types of RES integrated into a distribution network or the variation of grid strength.

The time given to complete the thesis was a single academic semester and therefore time was a constraint.

Load-shedding was a factor that affected the progress of the thesis as it occurred daily for several weeks throughout the semester.

1.7. Thesis Outline

The remainder of the thesis is organized as follows:

Chapter 2: Literature Review

This chapter presents the literature review that covers topics that are relevant to the thesis. These topics include the importance of renewable energy, basic concepts and functioning of PV cells, different types of cells, their applications, their growth in Africa and other countries, their benefits and challenges, the integration of PV systems in distribution networks, power quality, and techniques used by other researchers to optimize power quality in PV systems.

Chapter 3: Methodology

This chapter describes the steps that were taken to address the deliverables of the thesis. It describes the design of the distribution networks on DIgSILENT PowerFactory and the integration of solar PV systems. It further explains the methods used to measure and mitigate the power quality deviations of the system by properly selecting PV integration points. Finally, it outlines the case studies that were used to carry out the project.

Chapter 4: Results

This section presents the simulated results that were obtained from DIgSILENT and discusses them in detail. It includes voltage and frequency profiles of distribution networks before and after the integration of solar PV

systems. The deviations in the voltage and frequency profiles were analysed to assess how power quality is affected by the integration of PV systems in distribution networks. Furthermore, the voltage and frequency deviations for each case were calculated and the findings were discussed.

Chapter 5: Conclusions

This chapter concludes the thesis by summarising all the previous chapters and the accomplishments of the thesis. Moreover, it outlines the limitations of the thesis and suggests recommendations for future work in this field of study.

2. Literature Review

2.1. Introduction

The literature review presented in this chapter expands on topics that are relevant to the research project. It starts by explaining the need for renewable energy sources before outlining important photovoltaic (PV) cell concepts. The integration of PV systems in a distribution network is discussed and the Renewable Energy Grid Codes in South Africa for RES are outlined. The review further describes the power quality challenges experienced in a distribution network and the impact of PV system integration on power quality. Additionally, it discusses various methods used by researchers to assess these impacts and suggested approaches to reduce them. Table 2-1 describes the structure of the literature review.

Table 2-1: Summary of the topics covered in the literature review

Topic Reviewed	Items covered
1. Introduction	Introduction to the literature review
2. Renewable Energy	The importance of renewable energy is discussed
3. Introduction to Solar Photovoltaic Cells	A brief introduction to PV cells
4. Single PV Cell Module Theory	The mathematical model of a PV cell is described
5. Types of PV Cells	Monocrystalline, polycrystalline and thin film cells are described and compared
6. Benefits of PV Cells	The benefits of PV cells are outlined
7. General Applications of PV cells	General applications of PV cells are described
8. Applications of PV Cells in Africa and Other Countries	Applications of PV cells in Africa and other countries are discussed
9. Integration of PV Systems in Distribution Networks	The integration of PV cell systems in distribution networks is discussed
10. Grid Strength	The strength of grids is discussed
11. Renewable Energy Grid Codes in South Africa	South African grid codes for RES integration are outlined
12. Challenges Experienced by PV Plants	Challenges experienced by PV plants are outlined
13. Impact of Residential Solar PV System Integration on Power Quality	The impact of residential PV system integration is discussed
14. Power Quality Challenge Mitigation Technique	Various techniques used to mitigate power quality challenges are described
15. Conclusion	Summary of the topics discussed

2.2. Renewable Energy

The current demand for energy is increasing globally due to the increase in population and industrial activity. This is impacting the environment through global warming, and therefore the desire for environmentally friendly, renewable energy resources is growing. Conventional energy sources such as fossil fuels have been used as one of the primary sources of power for more than a hundred years, however, they are non-renewable and unsustainable. Additionally, the mining and burning of fossil fuels release large amounts of chemicals such as carbon dioxide into the atmosphere. This degrades the air quality which can adversely affect the health of humans, animals, and the environment. Governments and utility companies are under increased pressure to switch to renewable energy systems (RES) for residential and commercial use as a result of this. RES are environmentally friendly as they do not cause pollution and they have very few disadvantages. One of the most popular and rapidly developing RES is solar power, where energy production can be achieved through the use of solar photovoltaic cells.

2.3. Introduction to Solar Photovoltaic Cells

Solar photovoltaic cells are devices that convert solar radiation into electricity [7]. They consist of layered semiconducting material, the most common being silicon, due to its ability to convert solar radiation into electricity with high efficiency. Electricity is created and passed through the semiconducting material when the cells are penetrated by solar radiation and this phenomenon is known as the photoelectric effect. The amount of electricity produced and the efficiency of the system is dependent on temperature and irradiance, which is the amount of solar radiation that is incident on a surface [8].

2.4. Single PV Cell Module Theory

A single PV cell module's I-V curve describes its ability to convert energy under the present irradiance and temperature circumstances. It indicates the voltage and current values for which the cell module could be operated for certain irradiance and temperature levels. Figure 2-1 depicts the equivalent circuit of a single module of a diode-connected PV cell [1].

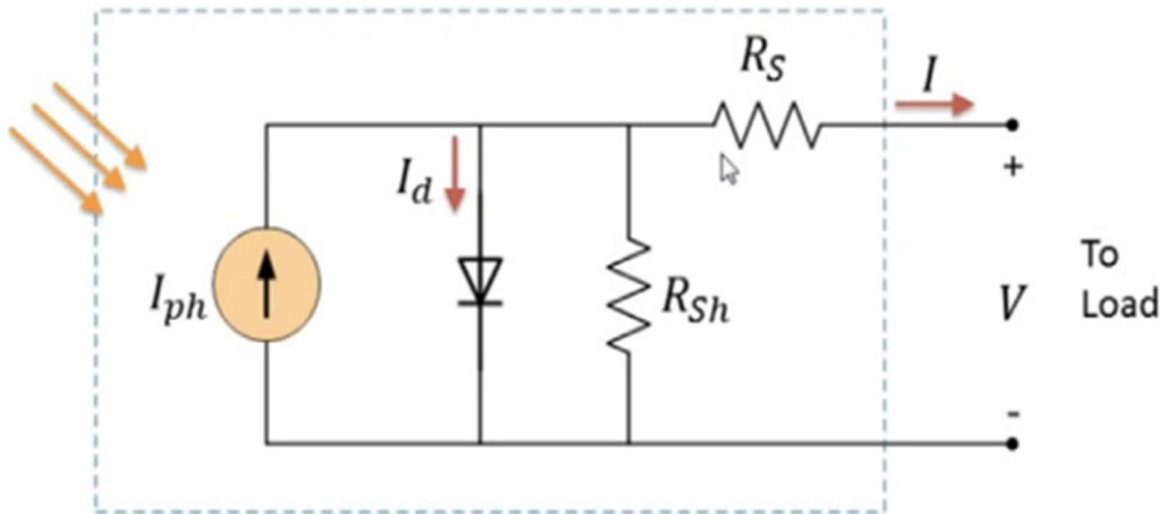


Figure 2-1: Diode-connected PV cell equivalent circuit [1]

The circuit in Figure 2-1 is mathematically described by Equation 2-1 below [1]:

$$I = I_{ph} - I_d - I_{R_{sh}} \quad (2-1)$$

Where:

I (A) is the total circuit current, I_{ph} (A) is the photon current, I_d (A) is the diode current and $I_{R_{sh}}$ (A) is the shunt resistor current [1].

Using Kirchoff's Law on the circuit in Figure 2-1, the equation describing the I-V characteristics is given by Equation 2-2 below [1]:

$$I = I_{ph} + I_o \left[e^{\frac{qV_t}{kT}} - 1 \right] + \frac{(V - IR_s)}{R_{sh}} \quad (2-2)$$

Where:

I_o (A) is dark saturation current, q (C) is electric charge, k is Steffan Boltzmann's constant, a is the ideality factor, V_t (V) is the thermal voltage, T ($^{\circ}$) is the temperature and R_s (Ω) is the series resistor current [1].

By setting the voltage V to zero and assuming that the resistance of R_s (Ω) is negligible, the short circuit current I_{sc} (A) can be determined using Equation 2-3 shown below [1].

$$I_{sc} = I_{ph} \quad (2-3)$$

The maximum possible voltage of the PV cell when there is no flow of external current V_{oc} (V) is dependent on temperature and material quality [1].

The fill factor (FF) of the PV cell is a quality measurement. It is the ratio of the maximum power of the cell to the product of V_{oc} (V) and I_{sc} (A). It is determined using Equation 2-4 below [1]:

$$FF = \frac{P_{max}}{(V_{oc})(I_{sc})} = \frac{(V_{max})(I_{max})}{(V_{oc})(I_{sc})} \quad (2-4)$$

The efficiency η of the PV cell is determined using Equation 2-5 below [1]:

$$\eta = \frac{P_{out}}{P_{in}} \rightarrow \eta_{max} = \frac{P_{max}}{P_{in}} = \frac{(V_{oc})(I_{sc})(FF)}{(I_t)(A_c)} \quad (2-5)$$

2.5. Types of PV Cells

There are many different types of PV cells that are categorized according to their semi-conducting material. The most commonly used types of PV cells are silicon-based due to silicon being abundant and non-toxic [9]. Commonly used silicon-based PV cells include monocrystalline silicon cells, polycrystalline silicon cells, and thin film or amorphous silicon solar cells [10].

2.5.1. Monocrystalline Silicon Cells

Monocrystalline silicon cells are made up of a single type of silicon crystal. They have the highest efficiency and power rating out of all other PV cells due to the structure of monocrystalline silicon, which allows for greater absorption of solar radiation. Unfortunately, this also makes them the most costly. Another advantage of monocrystalline silicon cells is that they are small in size and few panels are needed due to their high efficiency. They also have very long lifespans and can last up to 50 years [10].

2.5.2. Polycrystalline Silicon Cells

Unlike monocrystalline silicon cells, polycrystalline silicon cells are made from multiple types of silicon that have been fused. Polycrystalline silicon cells are less efficient and have a shorter lifespan than monocrystalline cells, however, they are cheaper to produce due to having a simpler manufacturing process [9].

2.5.3. Thin Film Solar Cells

Thin film or otherwise known as amorphous silicon solar cells, uses amorphous silicon as a semiconducting material. Although their manufacturing cost is much lower than crystalline silicon cells, they are also less efficient and have a shorter lifespan. However, their efficiency has improved over the last few years due to the improvement in technology and they are desirable due to their low material usage [11].

2.5.4. Comparison of PV Cells

Table 2-2 below compares the characteristics of each type of PV cell such as efficiency (%), performance, lifespan, and cost (USD/W_p).

Table 2-2: Comparison of the characteristics of each type of PV cell according to efficiency, performance, lifespan, and cost [3]/[4]

PV Cell Type	Monocrystalline Silicon Cell	Polycrystalline Silicon Cell	Thin Film Solar Cells
Efficiency (%)	25	21	10
Performance	Efficient when solar radiation is low	Less efficient when solar radiation is low	Least efficient when solar radiation is low
Life span	Up to 50 years	20 -35 years	10 - 20 years
Cost (USD/W _p)	0.185–0.380	0.160–0.290	0.200–0.320

2.6. Benefits of PV Cells

Photovoltaic cells are a renewable energy source because they rely on solar radiation which is freely available, abundant, and will never deplete. These devices work very efficiently and are able to convert solar radiation directly into DC voltage. They are extremely simple in operation, low maintenance in comparison to other energy-producing technology and have the potential to last for a very long time if maintained well. They can be described as modular systems which means that they can be easily expanded to fulfil the growing energy demand. They have a very low impact on the environment as they do not produce greenhouse gases that contribute to global warming and they also do not endanger human or animal life. Lastly, their simple design does not affect visual aesthetics or produce noise [8].

2.7. General Applications of PV Cells

Apart from being highly efficient and sustainable, one of the reasons that PV cells are growing in popularity is due to their wide variety of applications. One of the first applications of PV cells was in 1958, where they were used as a power source for orbiting satellites. Nowadays, they can be used as standalone systems in small, low-power devices such as calculators and digital wristwatches, or they can be combined to form a PV system where the electricity that is generated is used for lighting and everyday household electrical appliances in residential areas [12].

2.8. Applications of PV Cells in Africa and Other Countries

2.8.1. Africa

Access to electricity is one of the many challenges that people in Africa face and this has prompted the need for a reliable, affordable, and efficient energy source, such as solar power. The solar power industry is able to grow and thrive in Africa due to its exceptionally high availability of solar power which remains fairly constant throughout the year. More countries in Africa are starting to use the abundance of solar radiation to their advantage by building solar PV power plants to provide electricity to their residential households and community centres [13]. Countries in West Africa are amongst the poorest in Africa with the least access to

electricity. The potential for grid-connected PV systems on a large scale is being researched in these countries to help combat the electricity crisis [14]. The largest solar energy capacity in Africa is in South Africa and the use of PV cells is continuing to expand in provinces such as the Western Cape and Gauteng [13].

2.8.2. Other Countries

The leading solar energy producer is China, with other countries such as the United States and Japan following closely [6].

2.9. Integration of PV Systems in Distribution Networks

An electrical power system is composed of three networks: generation, transmission, and distribution. Generally, electricity is generated at the generation network before travelling through to the transmission network and finally reaching the distribution network. The project focuses on the integration of PV systems in distribution networks, which is responsible for distributing electricity for local use [13]. In such cases where the electricity is generated at the distribution network, it is referred to as distributed generation (DG). Apart from solar PV systems, other forms of DG include wind power and hydropower [15]. PV plants are integrated into a distribution network through power electronic converters and the system is typically composed of inverters, power meters, charge controllers, energy storage devices (batteries), and an electricity grid. When PV cells are interlinked, they are known as a PV array. Figure 2-2 below depicts the typical structure of a residential PV system connected to a utility grid, and includes a PV array, a DC-DC converter, and a DC-AC inverter [6][16].

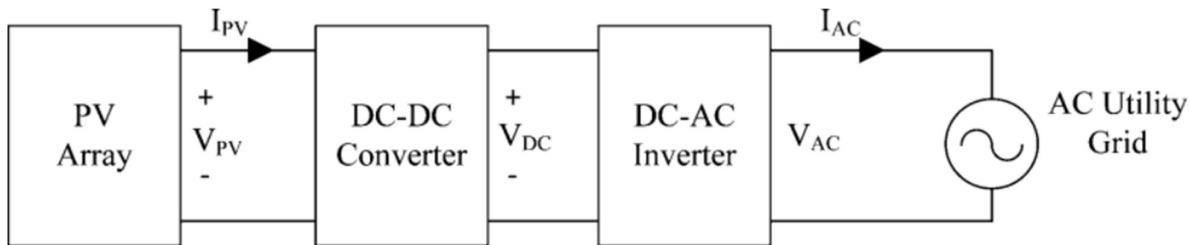


Figure 2-2: Residential PV system connected to the grid [2]

2.10. Grid Strength

The grid strength of power systems is determined by their impedance and/or inertia. Weak grids are characterized by either having high impedances or low inertia. This causes them to become more susceptible to voltage and frequency deviations making them unstable compared to stronger grids. Grid strengths are generally weakened in rural areas with high populations, or areas with poor electricity infrastructure. The grid strength of a DG system can be determined by using Equation 2-6 below to determine the short circuit ratio, which measures the impedance of the Point of Interface (POI) with the grid [17].

$$SCR_{POI} = \frac{S_{SC}}{P_n} \quad (2-6)$$

Where:

SCR_{POI} is the short-circuit ratio at the POI with the grid, S_{SC} is the Short Circuit Power (MW) and P_n is the output power of the DG plant (MW) [17].

2.11. Renewable Energy Grid Codes in South Africa

The South African Renewable Energy Grid Code acts as a guideline to help introduce DG systems into the grid. These guidelines require the point of connection (POC) of DG systems to operate within a specified voltage range. Table 2-3 below specifies the minimum voltage (U_{min}) and maximum voltages (U_{max}) for the POCs of DG systems for nominal voltages at the distribution level [5].

Table 2-3: Minimum (U_{min}) and maximum (U_{max}) voltages for the POCs of DG systems [5]

Nominal (Un)(kV)	U_{min} (p.u)	U_{max} (p.u)
132	0.9	1.0985
88	0.9	1.0985
66	0.9	1.0985
44	0.9	1.0800
33	0.9	1.0800
22	0.9	1.0800
11	0.9	1.0800

2.12. Challenges Experienced by PV Plants

Although PV plants have several advantages, new challenges are introduced when they are integrated into a distribution network. This section explores the challenges that are faced by PV plants. These challenges can affect the quality of power which will be discussed later in the review.

2.12.1. Fluctuations in Solar Radiation Availability

One of the challenges of PV plants is that they do not receive a constant input of solar radiation. This is due to the factors that influence the availability of solar radiation such as geographic location, season, time of day, the relative motion of the sun and the earth, and the changing atmospheric conditions such as cloud cover. Extensive research has shown that due to the fluctuation in the availability of solar radiation, residential solar PV system integration has an impact on the quality of power [8].

2.12.2. High Penetration Levels in LV Distribution Networks

Power quality challenges in PV systems also occur when penetration levels are too high for low-voltage (LV) distribution grids. Penetration levels refer to the ratio between the total quantity of PV system energy transmitted to a network and the PV system's total energy consumption which is shown in Equation 2-7 below. Penetration levels are categorized into low, medium, and high levels. High penetration levels cause deviations in frequency and voltage levels which can drastically impact the distribution grid by damaging the equipment and compromising the safety and reliability of the system. It is therefore important that this is monitored [6]. The penetration percentage (%) can be calculated using Equation 2-7 below [18]:

$$\text{PV Penetration \%} = \frac{\text{Peak PV Power}}{\text{Peak Load Apparent Power}} \times 100 \quad (2-7)$$

Where:

The Peak PV Power and the Peak Load Apparent Power are measured in Megawatts (MW) [18].

2.12.3. Lightning Strike Prone

The area taken up by PV plants is much greater than that of conventional electrical power plants. They are therefore at higher risk of being struck by lightning, especially in areas of high altitudes with minimal tall structures surrounding the area. Lightning strikes can damage equipment, reduce the efficiency of the system and affect the output power quality [19].

2.13. Impact of Residential Solar PV System Integration on Power Quality

This section will focus on the power quality issues that are experienced in distribution networks that occur as a result of the challenges outlined in the previous section. A power quality issue can refer to any difference or change in the magnitude and frequency of an ideal voltage sinusoidal wave [20]. The deviation percentage of voltage from a reference case can be calculated using Equation 2-8 below [21]. This equation can be used to determine the deviation of any measurable parameter.

$$\text{Deviation (\%)} = \frac{V_{\text{Measured}} - V_{\text{Reference}}}{V_{\text{Reference}}} \times 100\% \quad (2-8)$$

Where:

V_{Measured} is the voltage measured against the reference

$V_{\text{Reference}}$ is the reference voltage

The power quality issues that are most frequently experienced in a distribution network include overvoltage, voltage fluctuations, poor power factor, and harmonic distortion [7]. Each power quality issue is discussed in further detail.

2.13.1. Overvoltage

Overvoltage occurs when excess power is generated during periods when there are high penetrations of solar radiation but less demand for power. This challenge is more frequently faced in LV distribution grids where the power output is too high. This needs to be avoided as it can cause power outages and affect household appliances, thus, creating a safety hazard [7].

2.13.2. Voltage Fluctuations

The changing availability of solar radiation as discussed previously causes fluctuations in the voltage of PV systems. This is when the voltage deviates from its recommended value, which becomes problematic when the deviation occurs past its limiting range. Voltage fluctuations can lead to problems such as pink or flicker noise (type of electron noise), current surges, and energy losses in the distribution network [7].

2.13.3. Poor Power Factor

PV systems in the distribution network often operate at unity power factor i.e., when the current and voltage are in phase. PV systems can often reduce the power factor resulting in decreased power transmission [7].

2.13.4. Total Harmonic Distortion

Total Harmonic Distortion (THD) is one of the more prominent effects that need to be taken into account in PV systems. They create distortions in the voltage waveform which can create distortion in the power system which in turn causes the wires to overheat. Overheating of the line wires leads to a loss of energy and damage to equipment [7]. The THD of a system can be calculated using Equation 2-9 below [22]:

$$\text{THD} = \frac{\sqrt{\sum_{i=2}^{\max} M_i^2}}{M_1} \quad (2-9)$$

Where:

M_i is the i^{th} harmonic

2.14. Power Quality Challenge Mitigation Techniques

There are several mitigating techniques that have been researched and implemented in PV systems in different countries to reduce the effects of the power quality challenges mentioned previously. Each challenge has been researched and tested to observe how they impact power quality and appropriate solutions to reduce the effects were implemented and tested.

2.14.1. Overvoltage Mitigation Techniques

I. Real and Reactive Power Control

A study on real and reactive power control to mitigate overvoltage issues was done by L. Collins et al. from the University of Newcastle, Australia. Data was first collected from several PV system sites to use for simulations. The active power curtailment (APC) technique was applied which is when the PV system's output

power is manually decreased to below the maximum amount that PV system could be able to produce. The voltages were further controlled by the injection or absorption of reactive power [23]. This method proved to regulate the voltage of the system well and the network capacity was increased.

II. Three-Dimensional Modelling

The three-dimensional mathematical modelling technique was proposed by Qiuqin Sun et al. from the North China Electric Power University. This technique was used to prevent overvoltage due to lightning strikes in a PV system located on a mountain. The magnetic field induced by lightning and metal framing structure for the PV system was derived. The purpose of the frame was to direct the magnetic field in the opposite direction. The overvoltage of the PV system was successfully mitigated [19].

2.14.2. Voltage Fluctuation Mitigation Techniques

I. Electric Vehicles

The mitigation technique using electric vehicles (EVs) to reduce voltage fluctuations was implemented by N.B.G. Brinkel et al from Utrecht University in the Netherlands. The methodology of this investigation included carrying out a power flow analysis to assess the problems that occur in the grid distribution for cases in the years 2017, 2030, and 2050. The EV system was introduced and implemented by changing the charging procedure of EVs and the effectiveness of this strategy was observed. The final results of the study show that in 2030, there are few effects on the voltage levels however, in 2050, the effects on voltage levels are shown to become significantly higher and more problematic. It was also discovered that the intensity of the changing voltage levels was dependent on the location and configuration of the grid. Furthermore, the introduction of the EV system proved to stabilize the grid and reduce the amount of flicker noise, which is one of the problems associated with voltage fluctuations. Although this may have improved the PV system, it comes with extra expenses for the owners of EVs [24].

II. Geographical Dispersion

The geographical dispersion method to reduce voltage fluctuations was done by S. Shivashankar et al. from the University of Malaya. This method involved dispersing the PV power generation over a greater area. While significant suppression of fluctuations had occurred with this technique, it was also found that short-term fluctuations could not be effectively smoothed [25].

2.14.3. Poor Power Factor Mitigation Techniques

I. Control Design Using PSCAD

Haider Muaelou et al. from the Mansoura University in Egypt conducted a study on improving the power factor in PV systems using controller design to prevent the grid voltage from becoming unstable at the point of common coupling (PCC), which is the common point that connects to households that utilize the same power supply. The components of the PV system were first modelled and simulated on a power system simulation software called PSCAD and a controller was designed and implemented. The control design included a Maximum Power Point Tracking (MPPT) algorithm and controlling the injection of active and reactive power. The results showed that the controller was successful in improving the power factor [26].

2.14.4. Total Harmonic Distortion Mitigation Techniques

I. Transformer Integrated Filtering Method

Qianyi Liu et al. performed an investigation on managing the power quality of a PV power plant in China with a transformer-integrated filtering method. The plant contained a filtering station with two stages, where the first stage had a filtering transformer and the second stage had a grid transformer. It was discovered that the integration of the transformer improved the quality of power at the PCC and reduced the THD [27].

II. Predictive Adaptive Filter Method

An attempt to reduce THD in PV systems by using a predictive adaptive filter method was done by Liqaa Alhafadhi et al. from the National Chung Hsing University in China. Adaptive filters are digital filters that

have the ability to self-adjust their filter coefficients to changes in their input signal. A standalone PV system was used to test this method and a variety of algorithms namely the least mean square (LMS) algorithm, the normalized LMS (NLMS) algorithm, and the leaky LMS algorithm, were used to confirm its accuracy. Several filter values which varied in both length and step size were evaluated. The results showed that this approach can lower THD. The efficacy of the THD reduction is directly influenced by the step size and filter length, and the most effective combination was using small step sizes and long filters. The NLMS algorithm reduced THD the most effectively [28].

2.15. Conclusion

In conclusion, the literature review covered topics that are essential to the research project. Renewable energy sources such as solar power are cleaner and more sustainable alternatives to conventional energy sources such as fossil fuels. Methods for analysing the impact of residential solar PV system integration on power quality and suggested approaches to reduce these impacts were explored. The research by other researchers is strongly linked to the research project and therefore provides more insight and understanding of the topic. The knowledge gained from the literature review was used to help with approaching the project by aiding in the understanding of photovoltaic cells, how they are integrated into a distribution network and how power quality is affected by this. The information will also be used to help with the design of PV cell plants integrated into a distribution network.

3. Methodology

3.1. Introduction

This chapter describes the research methodology steps that were taken to address the deliverables of the thesis and plan the relevant case studies. The chapter starts by providing an overview of the design steps used to carry out the project and describes the selected software used. It moves on to modelling the components used to design the test system and further explains the design of the distribution network and the integration of solar Photovoltaic (PV) plants in detail. The parameters used to configure the components are presented the steps taken to simulate the voltage and frequency profiles of the distribution networks are described. Lastly, the case studies used to investigate the impact of residential solar PV system integration on power quality in a distribution network are explained. Table 3-1 summarizes the structure of the methodology.

Table 3-1: Steps describing the methodology

Step	Description
1	Introduction to the methodology
2	An overview of the design steps used to carry out the project
3	Selection of DIgSILENT PowerFactory as the simulation software
4	Modelling of the system components in DIgSILENT
5	The final design of the test system is shown and described
6	Simulation of the voltage and frequency profiles
7	Description of the case studies

3.2. Design Overview

This section provides an overview of the design steps taken to investigate the impact of residential solar PV system integration on power quality in a distribution network. DIgSILENT PowerFactory was used to design the test system and simulate voltage and frequency profiles of the distribution network for power quality analysis. The IEEE (Institute of Electrical and Electronics Engineers) 9-bus benchmark system represents a transmission system and was selected to be used as the base template. The IEEE 9-bus benchmark system was modified to accommodate two distribution networks that were connected using busbars and transformers, each with their own PV plant integrated into them. The parameters of all the components used to construct the system were configured appropriately to meet the system requirements. Each distribution network was stepped down to different distribution voltage levels, to observe how different distribution voltage levels affect the voltage and frequency profiles. Each system also consisted of a load, which was varied as the project required the consideration of high, medium, and low loads. The project also required the consideration of low medium and high penetration, and this was varied by changing the active power of the PV plants. A three-phase fault was applied to the system before a load flow analysis was done to assess the power quality of the system. Voltage and frequency profiles of the distribution networks at the points of integration (POI) were simulated for four different case studies, the first being a base case, which was used as a reference to compare the results of the remaining three cases.

3.3. Simulation Software Selection

DIgSILENT PowerFactory was chosen to be used for the project. It is one of the most popular power systems simulation software that allows for the analysis of generation, transmission, industrial, and in this case, distribution systems [29]. It provided all the necessary features that were needed to conduct the project such as the building of a distribution network, the application of solar PV cell systems, load flow analysis, and the simulation of voltage and frequency profiles. Additionally, it provided standardized model templates that were made use of in this project. For this project, DIgSILENT was used to construct distribution networks and

integrate PV plants to study how the voltage and frequency levels of the network behave under different penetration levels and varying loads.

3.4. Component Modelling in DgSILENT

This section describes the modelling of the components used to construct the distribution networks and the PV plants. The IEEE 9-bus benchmark system was selected to be used as a base template for the transmission system. The Western Electricity Coordinating Council (WECC) large-scale PV plant template was used to model the PV plants, which were integrated into the IEEE 9-bus benchmark system at distribution levels. The design also made use of additional buses, two-winding transformers, general loads, and an external grid. Each component is described in further detail and their parameter configurations are stated. Table 3-2 below shows the list of components used to construct the test system and their quantities.

Table 3-2: List of components used to construct the test system and their quantities

Component	Quantity
Busbars	2
Transformers	2
PV Plant Models	2
General Loads	2
External Grid	1

3.4.1. IEEE 9-bus Benchmark System

Figure 3-1 below shows the template of the IEEE 9-bus benchmark system.

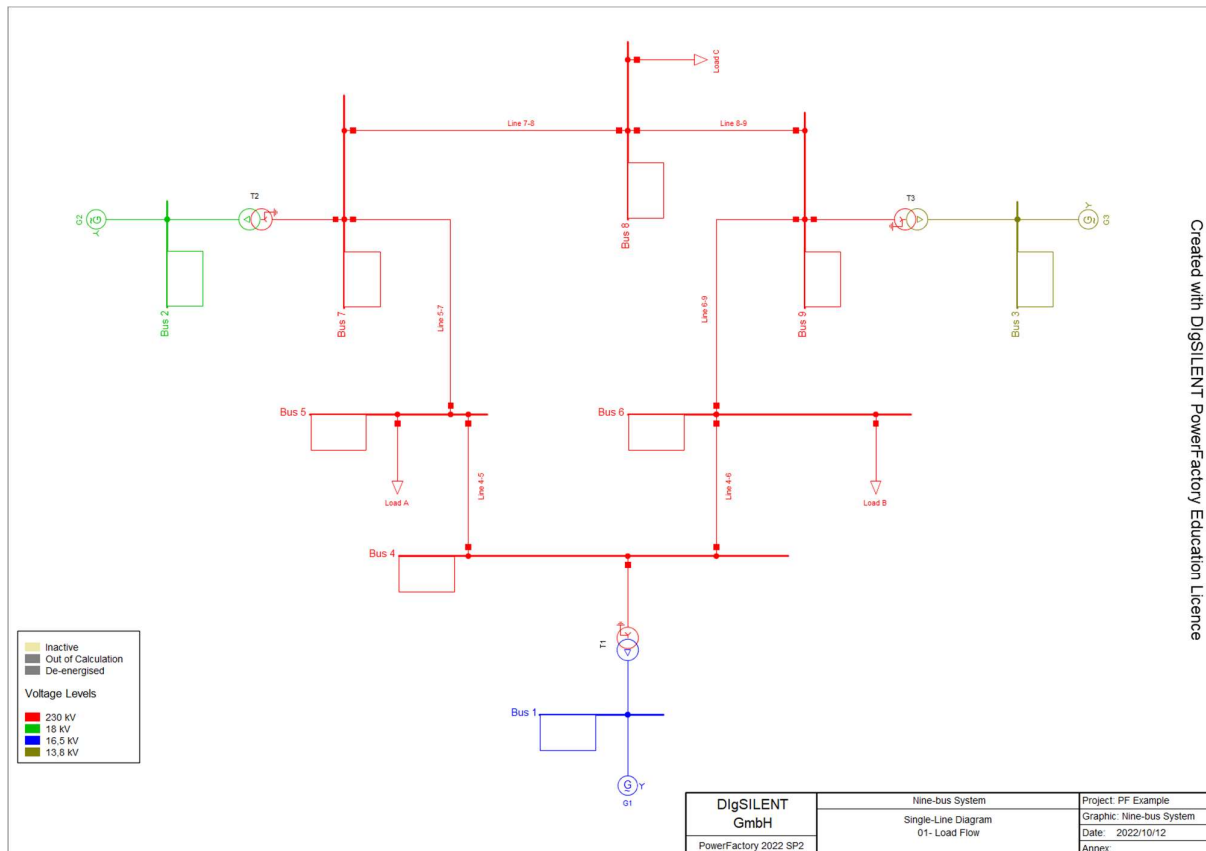


Figure 3-1: IEEE 9-bus benchmark system

IEEE bus benchmark systems are transmission systems based on IEEE standards that researchers employ to put new concepts and theories into practice [30]. The IEEE 9-bus benchmark system was considered for this

of the IEEE 9-bus system. Table 3-4 summarizes the parameter configurations of Transformer_1 and Transformer_2.

Table 3-4: Parameter configuration for Transformer_1 and Transformer_2

Transformer	Rated Power (MVA)	HV-Side (kV)	LV-Side (kV)	Frequency (Hz)
Transformer_1	250	230	66	60
Transformer_2	250	230	11	60

3.4.4. WECC Large-Scale PV Plant 110MVA 60Hz

Figure 3-2 below depicts the Western Electricity Coordinating Council (WECC) large-scale PV plant 110MVA 60Hz.

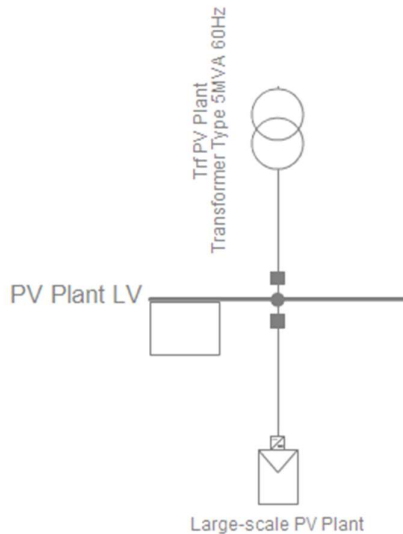


Figure 3-2: WECC Large-Scale PV Plant 110MVA 60Hz modelled in DIgSILENT

The WECC large-scale PV plant which operates at 110MVA and 60Hz was chosen to model the PV plants. This model and others are available for use on DIgSILENT and have been tested and certified according to the EPRI-written Renewable Energy Model Validation (REMV) tool, which reflects the WECC criteria. The models are standardized and the REMV tool has been verified against actual measurements [34]. This model was chosen because it operates at 60Hz, which corresponds to the frequency of the IEEE 9-bus system, and it also represents a large-scale plant, which is suitable for integration into power grids [21]. As seen in Figure 3-2, the model is composed of a transformer, a bus, and a static generator which represents the PV plant itself [35].

In the test system, one PV plant was integrated into each distribution network and was labelled PV_Plant_1 and PV_Plant_2. PV_Plant_1 was integrated into Distribution_1_66kV and PV_Plant_2 was integrated into Distribution_2_11kV. The reactive power of the PV plants was not modified as the system operates at a unity power factor, requiring the reactive power to be zero [36].

The project was required to consider low, medium, and high levels of penetration. The PV plants were specified active powers which determined the penetration levels of the system [37]. The complete system report generated on DIgSILENT after a load flow calculation of the system without the integration of PV plants, which can be seen in Figure A-1 in Appendix A, indicates that the system's total load is 465M. 50MW, 75MW,

external grid Short Circuit Power Sk''_{max} and Short Circuit Power Sk''_{min} were set to be 3000MVA and 1000MVA, respectively. Table 3-8 below specifies the parameter configuration of the external grid. [40]

Table 3-8: Parameter configuration of the external grid

Short Circuit Power Sk''_{max} (MVA)	Short Circuit Power Sk''_{min} (MVA)
3000	1000

3.5. Final Design of the Test System

This section describes the final design of the test system in detail. Figure 3-3 below depicts the test system which is composed of the modified model of the IEEE 9-bus benchmark system with the addition of distribution networks and the integration of PV plants.

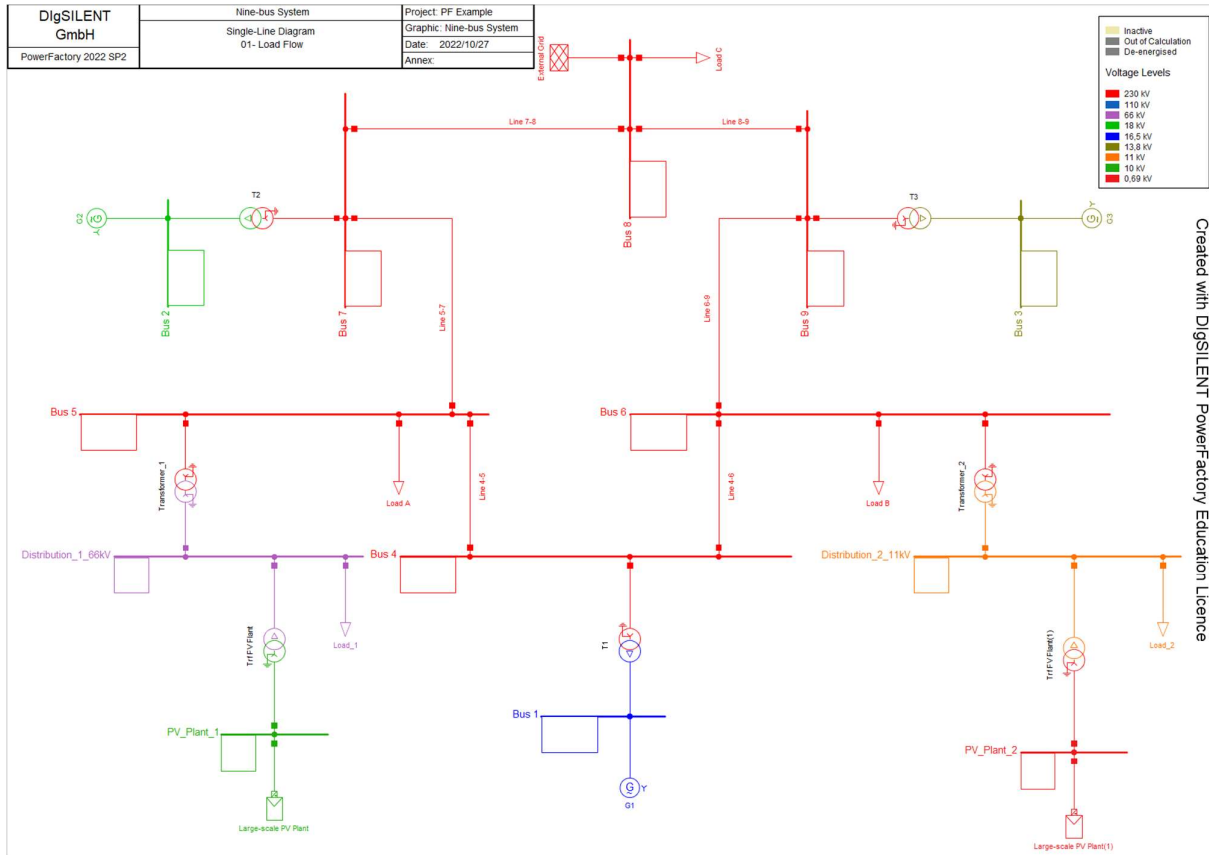


Figure 3-3: IEEE 9-bus system with distribution networks and PV plant integration

As seen in Figure 3-3, the IEEE 9-bus benchmark system was expanded on buses 5 and 6 which were available to accommodate distribution networks and the integration of PV plants. Transformer_1 was connected to Bus 5 and Transformer_2 was connected to Bus 6 to step down the voltage from the standard IEEE 9-bus system voltage of 230kV to voltages at distribution level. The distribution networks Distribution_1_66kV and Distribution_2_11kV were created by connecting busbars to the LV terminals of the transformers, and general loads were connected to these busbars. PV_Plant_1 and PV_Plant_2 were integrated into Distribution_1_66kV and Distribution_2_11kV, respectively. Load_1 and Load_2 were connected to Distribution_1_66kV and Distribution_2_11kV, respectively. Lastly, the external grid was connected to bus 8.

3.6. Simulation of Voltage and Frequency Profiles

This section describes the steps taken to generate voltage and frequency profiles for Distribution_1_66kV and Distribution_2_11kV to analyse their voltage and frequency deviations for different cases.

3.6.1. Three-phase Fault

A 3-phase fault is a short circuit event that was created on Distribution_1_66kV to analyse the power deviations of the system under this condition [33]. The fault was set to occur at time t=10s and cleared at t=10.5s. After time t=10.5s, the system would recover to its original state.

3.6.2. Load Flow Calculation

DIgSILENT allows users to conduct load flow calculations which were used to analyse the system in its initial state and ensure that the component parameters were configured appropriately. Once the initial conditions of the system were calculated, the simulation was executed for 100s. Voltage and frequency profiles were thus created for Distribution_1_66kV and Distribution_2_11kV for various cases, which will be discussed in the next section.

3.7. Planning of Case Studies

This section describes the planning of the case studies used to investigate the impact of residential solar PV system integration on power quality in a distribution network. Four case studies were planned, where Case 1 represented the base case. For each Case, both Distribution_1_66kV and Distribution_2_11kV were considered to observe how different distribution voltage levels impact power quality. All four cases considered loads and only Cases 2, 3, and 4 considered the integration of PV plants into the distribution networks with varying penetration levels. Load flow analyses were conducted for each case and the voltage and frequency profiles were obtained. These results were used to analyse the voltage and frequency deviations of the distribution networks for each case.

3.7.1. Case study 1 (Base): Testing of the system with a medium load (75MW) and without the integration of PV plants

The base case consisted of the IEEE 9-bus system without the integration of PV plants. The distribution networks Distribution_1_66kV and Distribution_2_11kV were connected to medium-powered loads of 75MW. Load flow analyses were conducted, and the voltage and frequency profiles of the system were obtained. The base case was used as a reference to compare the results of the other three cases, where the PV plants are integrated into the distribution networks and the penetration levels are varied.

3.7.2. Case study 2: Testing of the system with low loads (50MW) and with the integration of PV plants

The PV plants were integrated into the distribution networks. The system was tested with low loads of 50MW and with the integration of PV systems into each distribution network. The system was subjected to low (50MW), medium (75MW), and high (75MW) levels of penetration. Load flow analyses were conducted for each penetration level and the voltage and frequency profiles of the system were obtained.

3.7.3. Case study 3: Testing of the system with medium loads (75MW) and with the integration of PV plants

The PV plants were integrated into the distribution networks. The system was tested with medium loads of 75MW and with the integration of PV systems into each distribution network. The system was subjected to low (50MW), medium (75MW), and high (75MW) levels of penetration. Load flow analyses were conducted for each penetration level and the voltage and frequency profiles of the system were obtained.

3.7.4. Case study 4: Testing of the system with high loads (100MW) and with the integration of PV plants

The PV plants were integrated into the distribution networks. The system was tested with high loads of 100MW and with the integration of PV systems into each distribution network. The system was subjected to low (50MW), medium (75MW), and high (75MW) levels of penetration. Load flow analyses were conducted for each penetration level and the voltage and frequency profiles of the system were obtained.

4. Results and Discussion

Chapter 4 presents the results that were obtained from the simulations in DIgSILENT of the case studies and discusses them in detail. The voltage and frequency profiles of the base case are first presented, where medium loads of 75MW were connected to Distribution_1_66kV and Distribution_2_11kV. The results of this case were used as a reference for the results of the other cases to be compared. The remaining sections include the voltage and frequency profiles of Cases 2, 3, and 4, respectively. These graphs include the simulations of the base case for easy visualization of the deviations in voltage and frequency. On each profile, two intersection points were inserted at times $t=7\text{ s}$ and $t=35\text{ s}$. $T=7\text{ s}$ represents a point before the occurrence of the three-phase fault when the system was stable and operated normally. $T=35\text{ s}$ represents a point after the occurrence of the three-phase fault, once the system had stabilized. This was done to compare the voltage and frequency deviations of the distribution systems before and after the occurrence of the fault event. The intersection points displayed the magnitudes of voltages (p.u.) and frequencies (Hz) so that they could be easily identified and used for the deviation calculations. The voltage and frequency deviations were calculated using Equation 2-8 which was presented in Section 2.13 of the literature review. The voltage and frequency deviation calculations were done on a Microsoft Excel spreadsheet which is shown in Figure B-1 in Appendix B. Furthermore, the voltage and frequency magnitudes and the deviation values were summarized in tables which can be seen at the end of this chapter. Additionally, the voltage and frequency magnitudes of the distribution systems were compared to South African Renewable Energy Grid Codes which was discussed in Section 2.10 of the literature review.

4.1. Case Study 1 (Base): Voltage and frequency simulations of the system with medium loads (75MW) and without the integration of Solar PV plants (no penetration)

4.1.1. Voltage Profile

Figure 4-1 below depicts the voltage profiles for Distribution_1_66kV and Distribution_2_11kV of the base case where the system consisted of medium loads (75MW) and did not include the integration of PV plants.

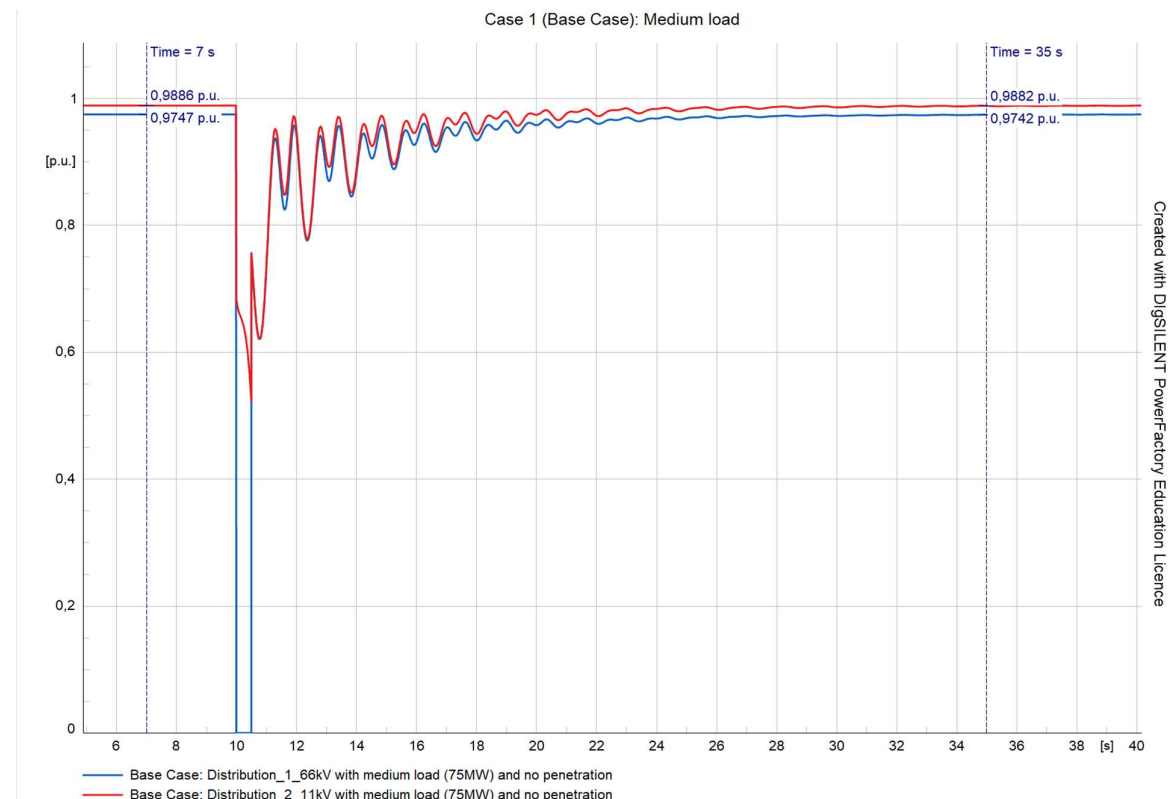


Figure 4-1: Voltage profile for the base case

The analysis of Figure 4-1 is as follows:

Between times $0 < t < 10$ s, the system operates normally before the occurrence of the three-phase fault.

The voltage magnitude of Distribution_1_66kV at $t=7$ s is 0,9747p.u and the voltage magnitude of Distribution_2_11kV at $t=7$ s is 0,9886p.u. These are base case values that were used as a reference to compare the voltage magnitudes at time $t=7$ s for Cases 2, 3, and 4.

The three-phase fault occurs at $t=10$ s.

Between $10 < t < 10.5$ s the system experienced oscillation as it was recovering from the three-phase fault that was created.

At $t=35$ s the system has returned to its stable state again. The voltage magnitude of Distribution_1_66kV at $t=35$ s is 0,9742p.u and The voltage magnitude of Distribution_2_11kV at $t=35$ s is 0,9882p.u. These are base case values that were used as a reference to compare the voltage magnitudes at time $t=35$ s from Cases 2, 3, and 4. These values do not match those from time $t=7$ s, as the system did not fully recover from the fault.

4.1.2. Frequency Profile

Figure 4-2 depicts the frequency profiles for Distribution_1_66kV and Distribution_2_11kV of the base case where the system consisted of medium loads (75MW) and did not include the integration of PV plants.

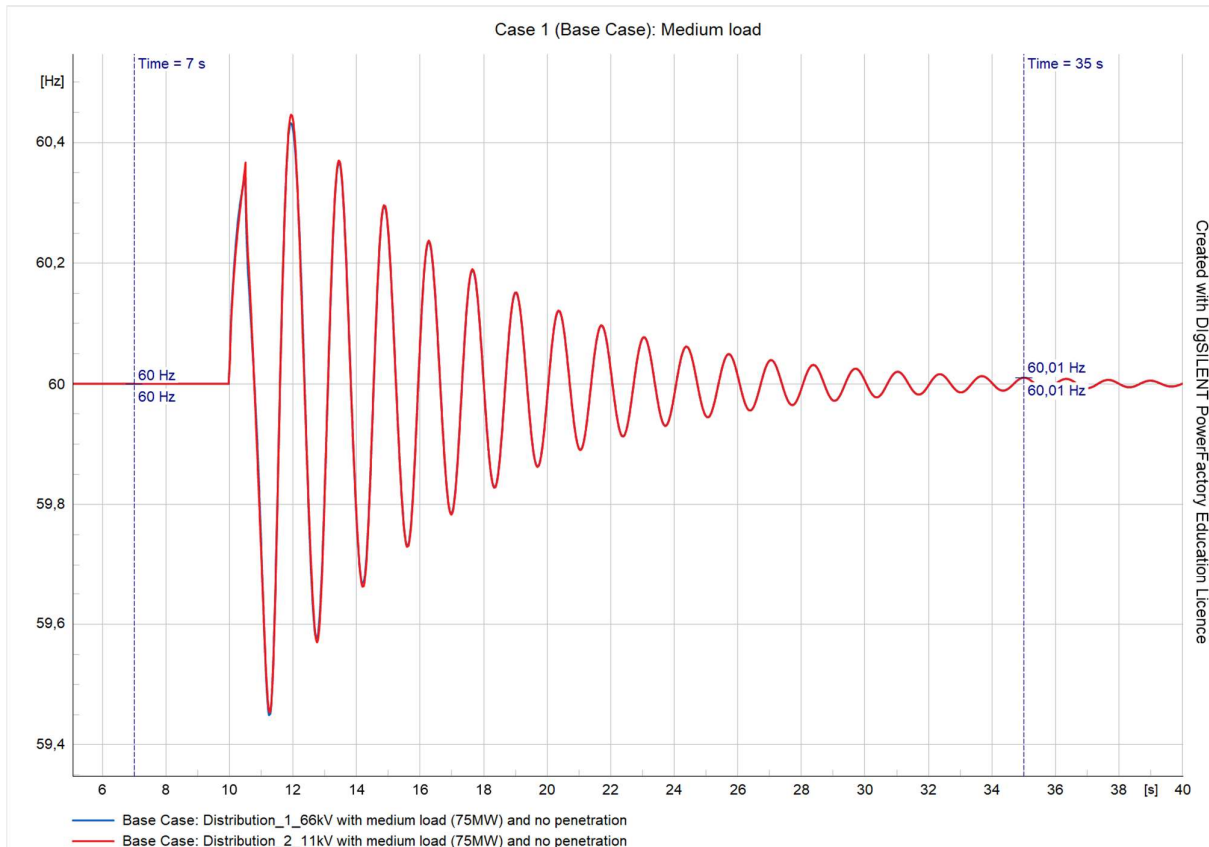


Figure 4-2: Frequency profile for the base case

The analysis of Figure 4-2 is as follows:

Between times $0 < t < 10$ s, the system operates normally before the occurrence of the three-phase fault.

The frequency magnitude of Distribution_1_66kV at $t=7$ s is 60Hz and the frequency magnitude of Distribution_2_11kV at $t=7$ s is also 60Hz. These are base case values that were used as a reference to compare the frequency magnitudes at time $t=7$ s from Cases 2, 3, and 4.

The three-phase fault occurs at $t=10$ s.

Between $10 < t < 10.5$ s the system experienced oscillation as it was recovering from the three-phase fault that was created.

At $t=35$ s the system has returned to its stable state again. The frequency magnitude of Distribution_1_66kV at $t=35$ s is 60.01Hz and the frequency magnitude of Distribution_2_11kV at $t=7$ s is also 60.01Hz. These are base case values that were used as a reference to compare the frequency magnitudes at time $t=35$ s from Cases 2, 3, and 4. These values do not match those from time $t=7$ s, as the system did not fully recover from the fault.

4.2. Case Study 2: Voltage and frequency simulations of the system with low loads (50MW) and with varying levels of penetration

4.2.1 Low Penetration Levels

I. Voltage Profile

Figure 4-3 depicts the voltage profiles for Distribution_1_66kV and Distribution_2_11kV of Case 2 where the system consisted of low loads (50MW) and low levels of penetration (50MW) applied. The base case voltage profiles for Distribution_1_66kV and Distribution_2_11kV are also included.

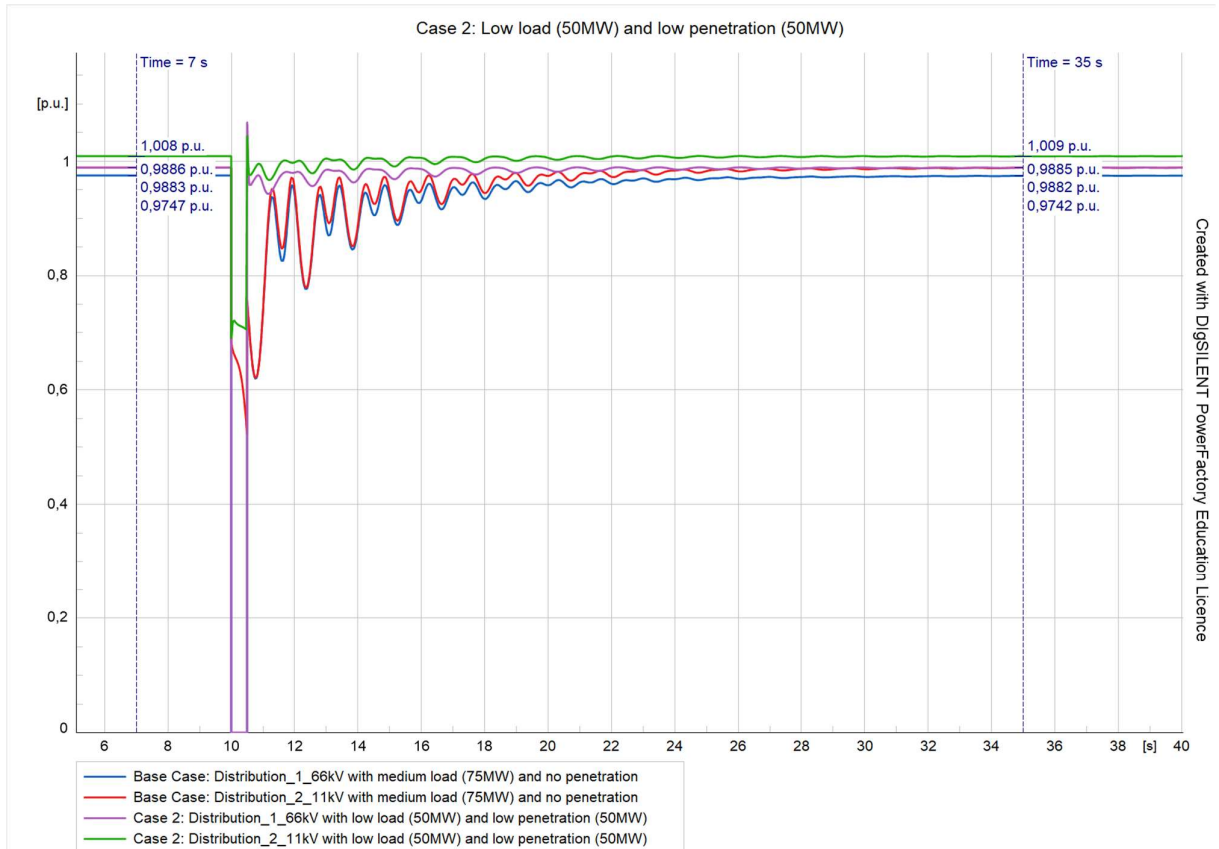


Figure 4-3: Voltage profile for Case 2 with low penetration levels

The analysis of Figure 4-3 is as follows:

Between times $0 < t < 10$ s, the system operates normally before the occurrence of the three-phase fault.

The voltage magnitude of Distribution_1_66kV at t=7s is 0,9883p.u and the voltage magnitude of Distribution_2_11kV at t=7s is 1,008p.u.

The three-phase fault occurs at t=10s.

Between 10< t < 10.5s the system experienced oscillation as it was recovering from the three-phase fault that was created.

At t=35s the system has returned to its stable state again. The voltage magnitude of Distribution_1_66kV at t=35s is 0,9885p.u and the voltage magnitude of Distribution_2_11kV at t=35s is 1,009p.u. These values do not match those from time t=7s, as the system did not fully recover from the fault.

The voltage magnitudes from this case for both times t=7s and t=35s differ from those of the base case, which indicates that there is voltage deviation. Using Equation 2-8, the voltage deviation for Distribution_1_66kV at t=7s was calculated to be 1,40% and at t=35s it was calculated to be 1,47%.

The voltage deviation for Distribution_2_11kV at t=7s was calculated to be 1.96% and at t=35s it was calculated to be 2.1%.

II. Frequency Profile

Figure 4-4 depicts the frequency profiles for Distribution_1_66kV and Distribution_2_11kV where the system consisted of low loads (50MW) and low levels of penetration (50MW) applied. The base case frequency profiles for Distribution_1_66kV and Distribution_2_11kV are also included.

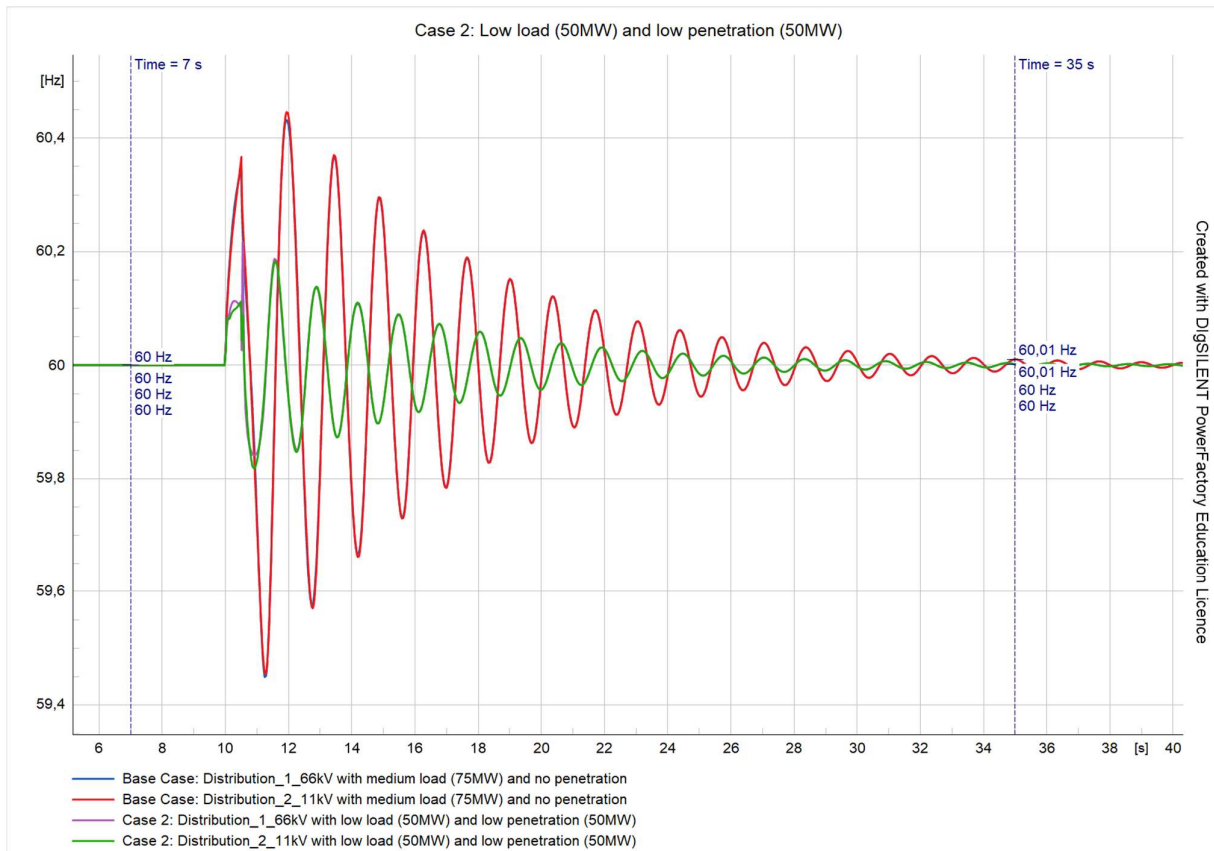


Figure 4-4: Frequency profile for Case 2 with low penetration levels

The analysis of Figure 4-4 is as follows:

Between times 0<t<10s, the system operates normally before the occurrence of the three-phase fault.

The frequency magnitude of Distribution_1_66kV at t=7s is 60Hz and the frequency magnitude of Distribution_2_11kV at t=7s is 60Hz.

The three-phase fault occurs at t=10s.

Between 10< t < 10.5s the system experienced oscillation as it was recovering from the three-phase fault that was created.

At t=35s the system has returned to its stable state again. The frequency magnitude of Distribution_1_66kV at t=35s is 60Hz and the frequency magnitude of Distribution_2_11kV at t=35s is 60Hz. These values do not match those from time t=7s, as the system did not fully recover from the fault.

The frequency magnitudes from this case for both times t=7s and t=35s differ from those of the base case, which indicates that there is frequency deviation. Using Equation 2-8 the frequency deviation for Distribution_2_11kV at t=7s and t=35s was calculated to be 0%.

The frequency deviation for Distribution_2_11kV at t=7s and t=35s was calculated to be -0.02%.

4.2.2. Medium Penetration Levels

I. Voltage Profile

Figure 4-5 depicts the voltage profiles for Distribution_1_66kV and Distribution_2_11kV where the system consisted of low loads (50MW) and medium levels of penetration (75MW) applied. The base case voltage profiles for Distribution_1_66kV and Distribution_2_11kV are also included.

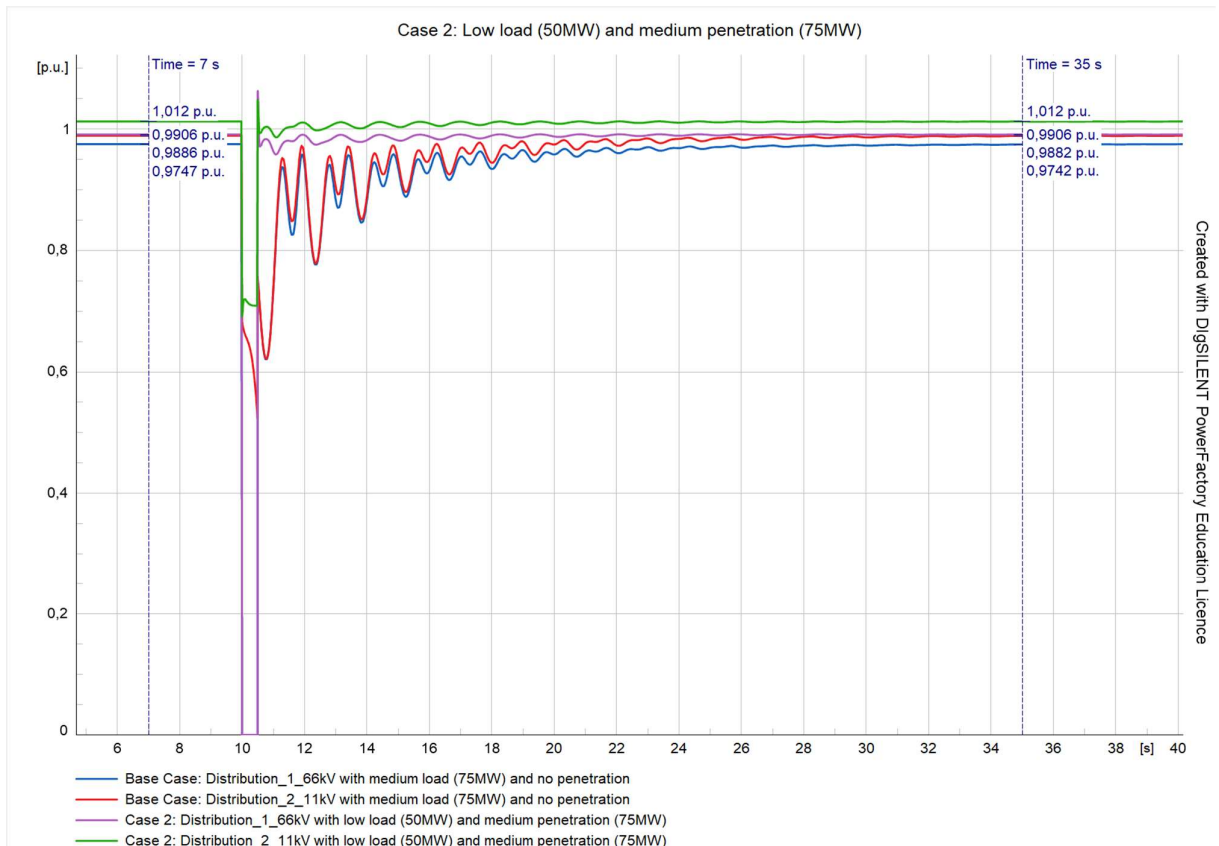


Figure 4-5: Voltage profile for Case 2 with medium penetration levels

The analysis of Figure 4-5 is as follows:

Between times $0 < t < 10$ s, the system operates normally before the occurrence of the three-phase fault.

The voltage magnitude of Distribution_1_66kV at $t=7$ s is 0,9906p.u and the voltage magnitude of Distribution_2_11kV at $t=7$ s is 1,012p.u.

The three-phase fault occurs at $t=10$ s.

Between $10 < t < 10.5$ s the system experienced oscillation as it was recovering from the three-phase fault that was created.

At $t=35$ s the system has returned to its stable state again. The voltage magnitude of Distribution_1_66kV at $t=35$ s is 0,9906p.u and the voltage magnitude of Distribution_2_11kV at $t=35$ s is 1,012p.u. These values do not match those from time $t=7$ s, as the system did not fully recover from the fault.

The voltage magnitudes from this case for both times $t=7$ s and $t=35$ s differ from those of the base case, which indicates that there is voltage deviation. Using Equation 2-8, the voltage deviation for Distribution_1_66kV at $t=7$ s was calculated to be 1,63% and at $t=35$ s it was calculated to be 1,68%.

The voltage deviation for Distribution_2_11kV at $t=7$ s was calculated to be 2,37% and at $t=35$ s it was calculated to be 2,41%.

II. Frequency Profile

Figure 4-6 depicts the frequency profiles for Distribution_1_66kV and Distribution_2_11kV where the system consisted of low loads (50MW) and medium levels of penetration (75MW) applied. The base case frequency profiles for Distribution_1_66kV and Distribution_2_11kV are also included.

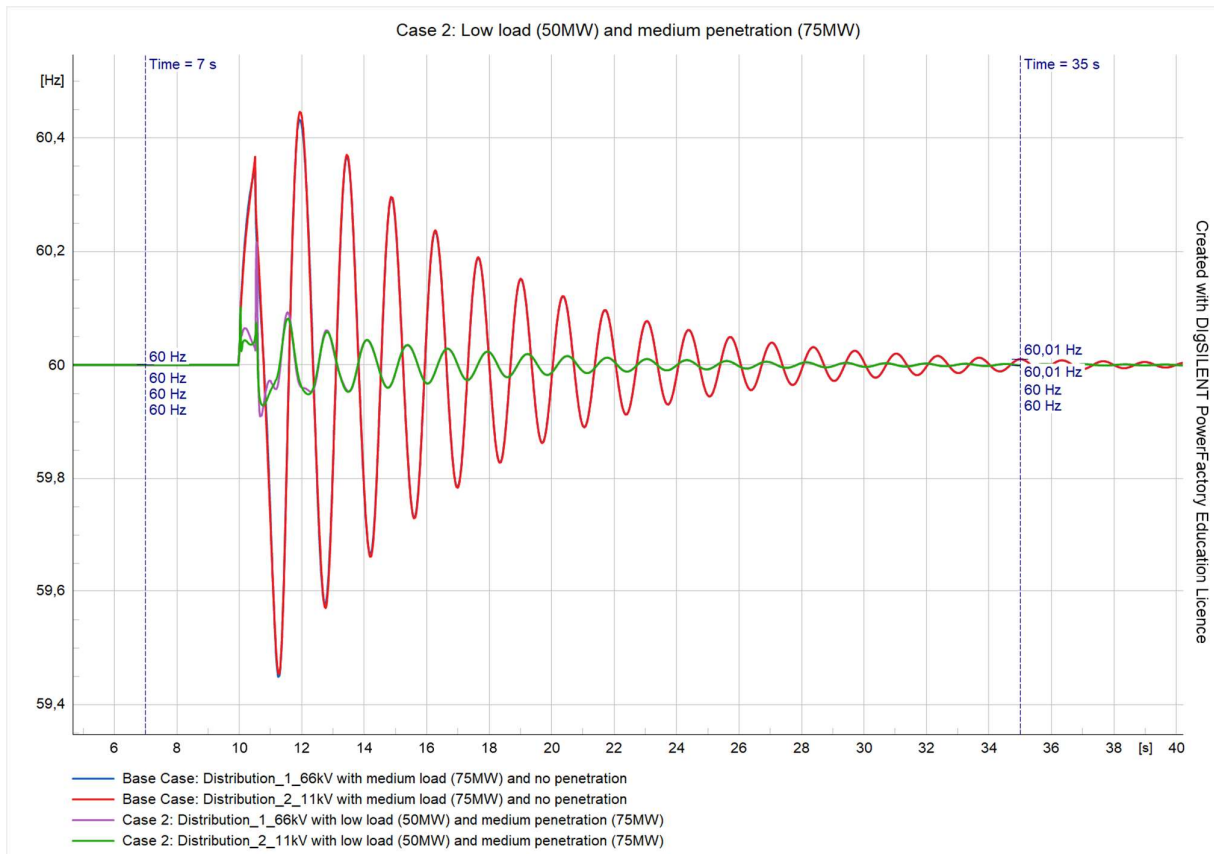


Figure 4-6: Frequency profile for Case 2 with medium penetration levels

The analysis of Figure 4-6 is as follows:

Between times $0 < t < 10$ s, the system operates normally before the occurrence of the three-phase fault.

The frequency magnitude of Distribution_1_66kV at $t=7$ s is 60Hz and the frequency magnitude of Distribution_2_11kV at $t=7$ s is 60Hz.

The three-phase fault occurs at $t=10$ s.

Between $10 < t < 10.5$ s the system experienced oscillation as it was recovering from the three-phase fault that was created.

At $t=35$ s the system has returned to its stable state again. The frequency magnitude of Distribution_1_66kV at $t=35$ s is 60Hz and the frequency magnitude of Distribution_2_11kV at $t=35$ s is 60Hz. These values do not match those from time $t=7$ s, as the system did not fully recover from the fault.

The frequency magnitudes from this case for both times $t=7$ s and $t=35$ s differ from those of the base case, which indicates that there is frequency deviation. Using Equation 2-8 the frequency deviation for Distribution_2_11kV at $t=7$ s and $t=35$ s was calculated to be 0%.

The frequency deviation for Distribution_2_11kV at $t=7$ s and $t=35$ s was calculated to be -0.02%.

4.2.3. High Penetration Levels

I. Voltage Profile

Figure 4-7 depicts the voltage profiles for Distribution_1_66kV and Distribution_2_11kV where the system consisted of low loads (50MW) and high levels of penetration (100MW) were applied. The base case voltage profiles for Distribution_1_66kV and Distribution_2_11kV are also included.

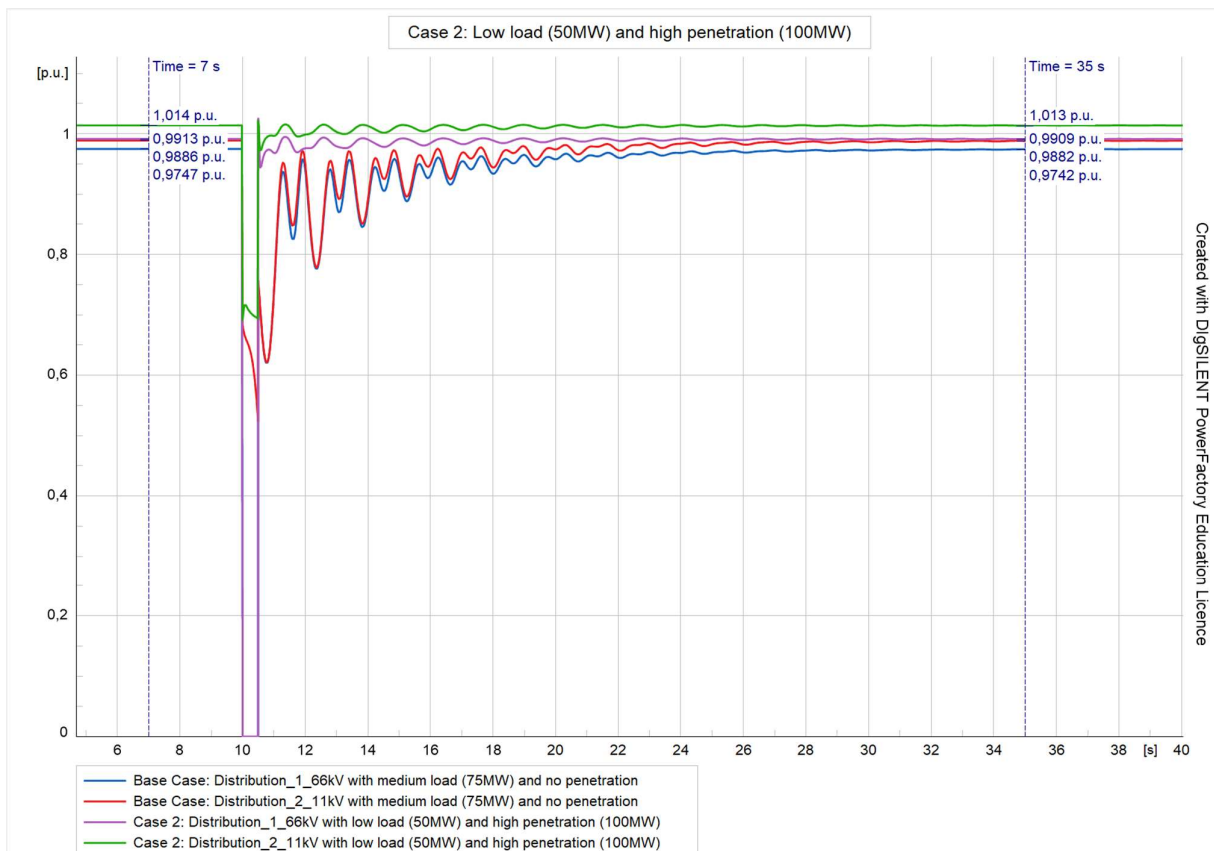


Figure 4-7: Voltage profile for Case 2 with high penetration levels

The analysis of Figure 4-7 is as follows:

Between times $0 < t < 10$ s, the system operates normally before the occurrence of the three-phase fault.

The voltage magnitude of Distribution_1_66kV at $t=7$ s is 0,9913p.u and the voltage magnitude of Distribution_2_11kV at $t=7$ s is 1,014p.u.

The three-phase fault occurs at $t=10$ s.

Between $10 < t < 10.5$ s the system experienced oscillation as it was recovering from the three-phase fault that was created.

At $t=35$ s the system has returned to its stable state again. The voltage magnitude of Distribution_1_66kV at $t=35$ s is 0,9909p.u and the voltage magnitude of Distribution_2_11kV at $t=35$ s is 1,013p.u. These values do not match those from time $t=7$ s, as the system did not fully recover from the fault.

The voltage magnitudes from this case for both times $t=7$ s and $t=35$ s differ from those of the base case, which indicates that there is voltage deviation. Using Equation 2-8, the voltage deviation for Distribution_1_66kV at $t=7$ s was calculated to be 1,70% and at $t=35$ s it was calculated to be 1,71%.

The voltage deviation for Distribution_2_11kV at $t=7$ s was calculated to be 2,57% and at $t=35$ s it was calculated to be 2,51%.

II. Frequency Profile

Figure 4-8 depicts the frequency profiles for Distribution_1_66kV and Distribution_2_11kV where the system consisted of low loads (50MW) and high levels of penetration (100MW) applied. The base case frequency profiles for Distribution_1_66kV and Distribution_2_11kV are also included.

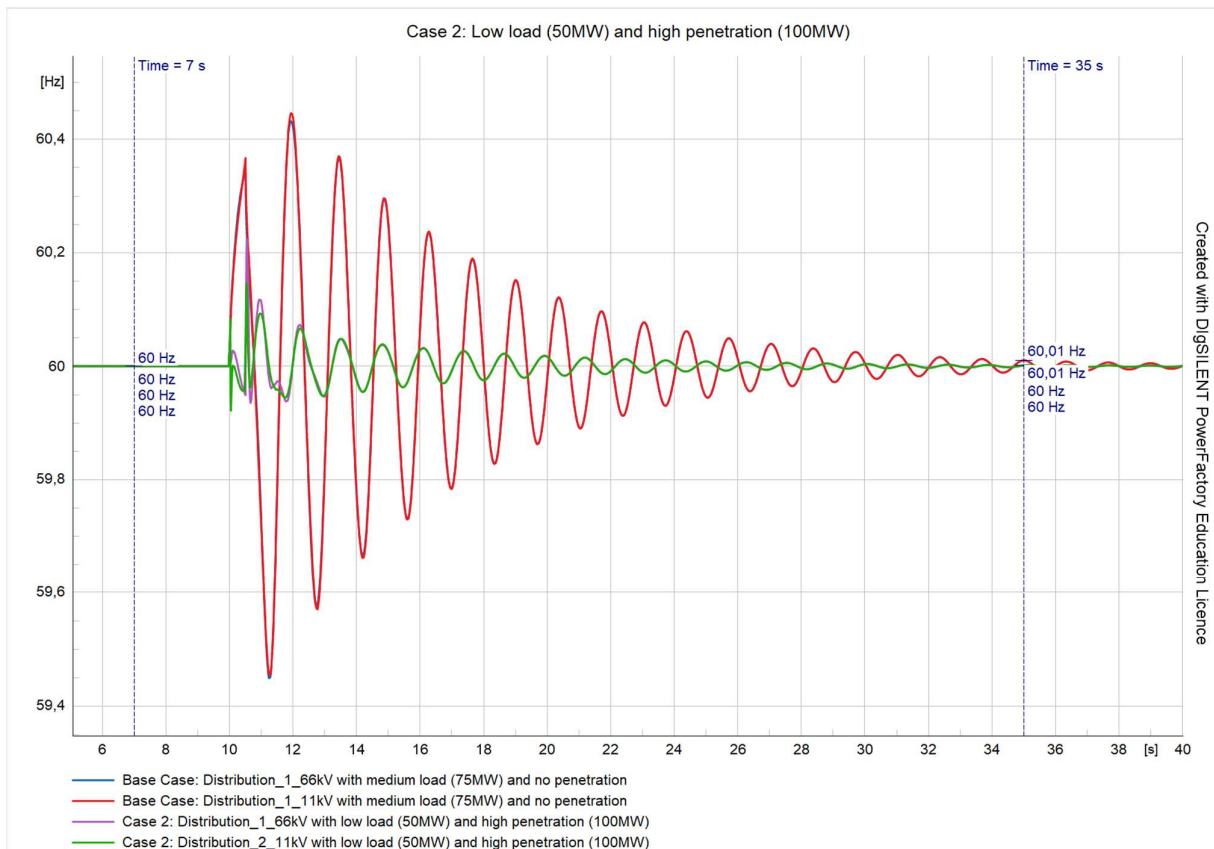


Figure 4-8: Frequency profile for Case 2 with high penetration levels

The analysis of Figure 4-8 is as follows:

Between times $0 < t < 10$ s, the system operates normally before the occurrence of the three-phase fault.

The frequency magnitude of Distribution_1_66kV at $t=7$ s is 60Hz and the frequency magnitude of Distribution_2_11kV at $t=7$ s is 60Hz.

The three-phase fault occurs at $t=10$ s.

Between $10 < t < 10.5$ s the system experienced oscillation as it was recovering from the three-phase fault that was created.

At $t=35$ s the system has returned to its stable state again. The frequency magnitude of Distribution_1_66kV at $t=35$ s is 60Hz and the frequency magnitude of Distribution_2_11kV at $t=35$ s is 60Hz. These values do not match those from time $t=7$ s, as the system did not fully recover from the fault.

The frequency magnitudes from this case for both times $t=7$ s and $t=35$ s differ from those of the base case, which indicates that there is frequency deviation. Using Equation 2-8 the frequency deviation for Distribution_2_11kV at $t=7$ s and $t=35$ s was calculated to be 0%.

The frequency deviation for Distribution_2_11kV at $t=7$ s and $t=35$ s was calculated to be -0.02%.

4.3. Case Study 3: Voltage and frequency simulations of the system with medium loads (75MW) and with varying levels of penetration

4.3.1. Low Penetration Levels

I. Voltage Profile

Figure 4-9 depicts the voltage profiles for Distribution_1_66kV and Distribution_2_11kV where the system consisted of medium loads (75MW) and low levels of penetration (50MW) were applied. The base case voltage profiles for Distribution_1_66kV and Distribution_2_11kV are also included.

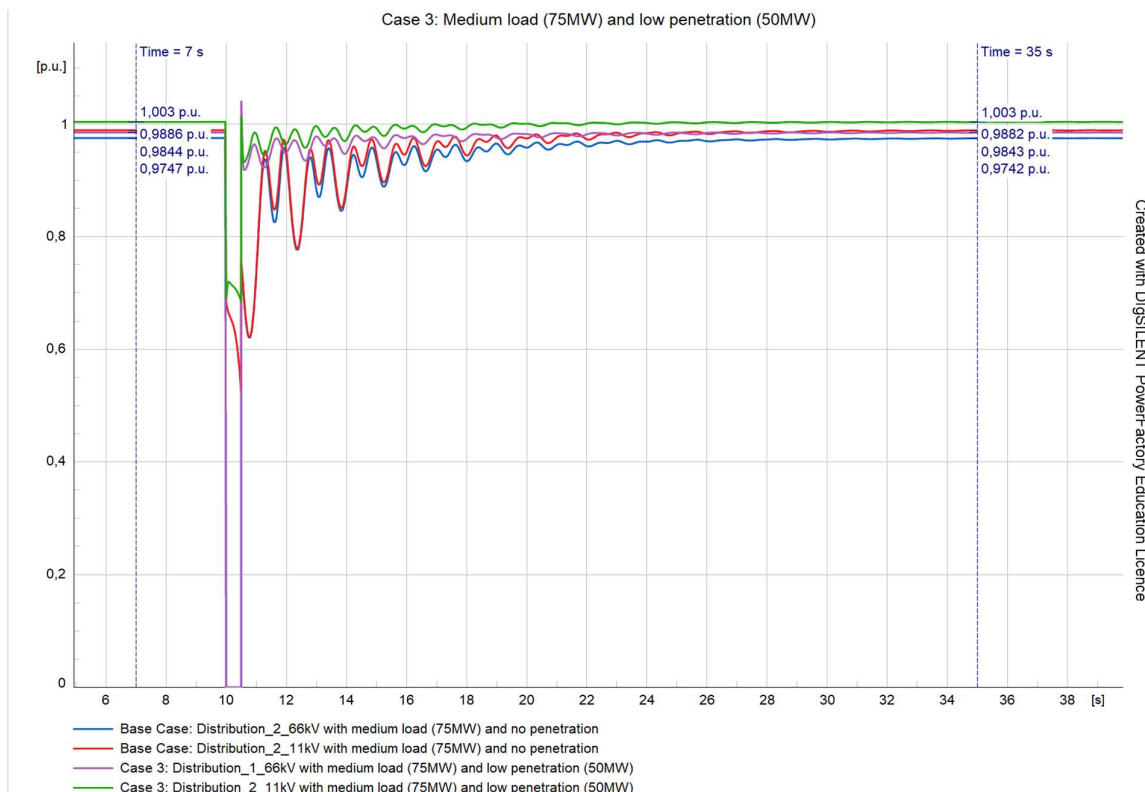


Figure 4-9: Voltage profile for Case 3 with low penetration levels

The analysis of Figure 4-9 is as follows:

Between times $0 < t < 10$ s, the system operates normally before the occurrence of the three-phase fault.

The voltage magnitude of Distribution_1_66kV at $t=7$ s is 0.9844p.u and the voltage magnitude of Distribution_2_11kV at $t=7$ s is 1.003p.u.

The three-phase fault occurs at $t=10$ s.

Between $10 < t < 10.5$ s the system experienced oscillation as it was recovering from the three-phase fault that was created.

At $t=35$ s the system has returned to its stable state again. The voltage magnitude of Distribution_1_66kV at $t=35$ s is 0.9843p.u and the voltage magnitude of Distribution_2_11kV at $t=35$ s is 1.003p.u. These values do not match those from time $t=7$ s, as the system did not fully recover from the fault.

The voltage magnitudes from this case for both times $t=7$ s and $t=35$ s differs to those of the base case, which indicates that there is voltage deviation. Using Equation 2-8, the voltage deviation for Distribution_1_66kV at $t=7$ s was calculated to be 1.00% and at $t=35$ s it was calculated to be 1.04%.

The voltage deviation for Distribution_2_11kV at $t=7$ s was calculated to be 1.46% and at $t=35$ s it was calculated to be 1.50%.

II. Frequency Profile

Figure 4-10 depicts the frequency profiles for Distribution_1_66kV and Distribution_2_11kV where the system consisted of medium loads (75MW) and low levels of penetration (50MW) was applied. The base case frequency profiles for Distribution_1_66kV and Distribution_2_11kV are also included.

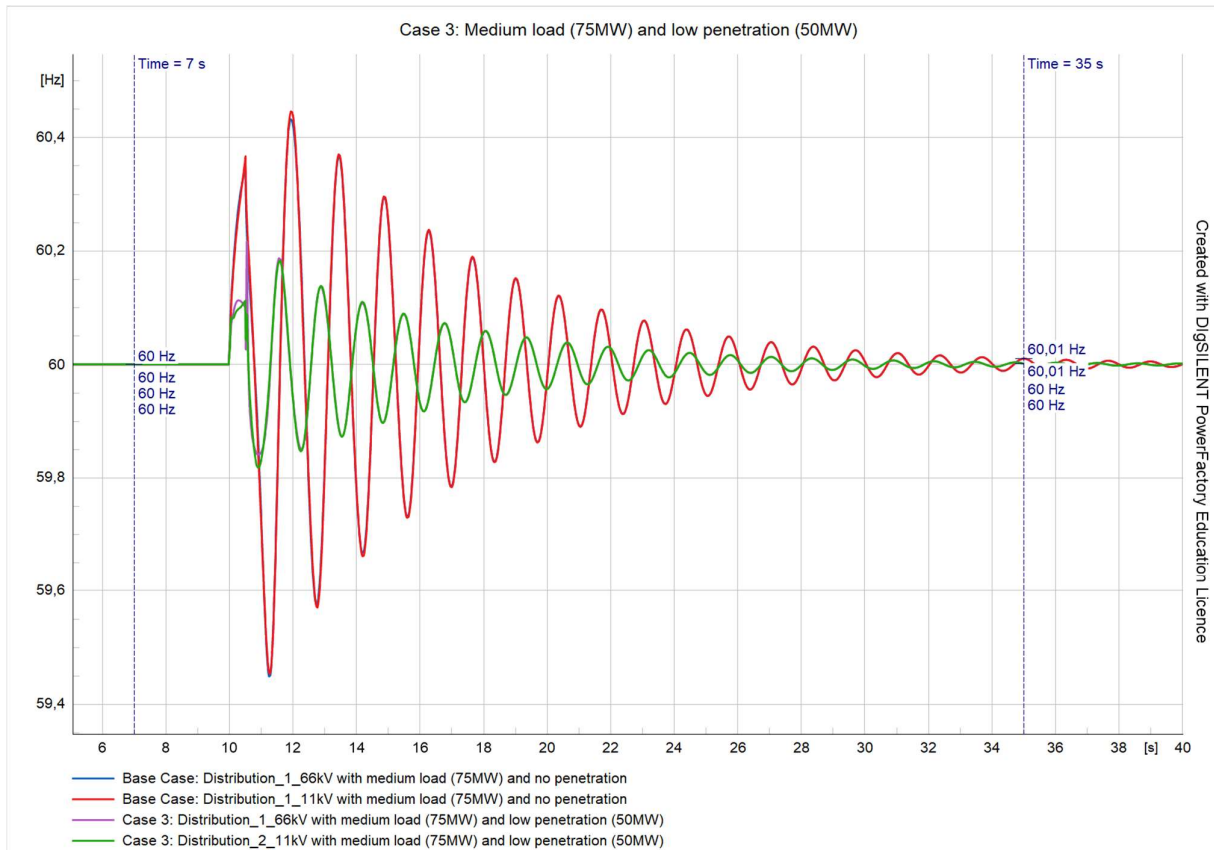


Figure 4-10: Frequency profile for Case 3 with low penetration levels

The analysis of Figure 4-10 is as follows:

Between times $0 < t < 10$ s, the system operates normally before the occurrence of the three-phase fault.

The frequency magnitude of Distribution_1_66kV at $t=7$ s is 60Hz and the frequency magnitude of Distribution_2_11kV at $t=7$ s is 60Hz.

The three-phase fault occurs at $t=10$ s.

Between $10 < t < 10.5$ s the system experienced oscillation as it was recovering from the three-phase fault that was created.

At $t=35$ s the system has returned to its stable state again. The frequency magnitude of Distribution_1_66kV at $t=35$ s is 60Hz and the frequency magnitude of Distribution_2_11kV at $t=35$ s is 60Hz. These values do not match those from time $t=7$ s, as the system did not fully recover from the fault.

The frequency magnitudes from this case for both times $t=7$ s and $t=35$ s differ from those of the base case, which indicates that there is frequency deviation. Using Equation 2-8 the frequency deviation for Distribution_2_11kV at $t=7$ s and $t=35$ s was calculated to be 0%.

The frequency deviation for Distribution_2_11kV at $t=7$ s and $t=35$ s was calculated to be -0.02%.

4.3.2. Medium Penetration Levels

I. Voltage Profile

Figure 4-11 depicts the voltage profiles for Distribution_1_66kV and Distribution_2_11kV where the system consisted of medium loads (75MW) and medium levels of penetration (75MW) were applied. The base case voltage profiles for Distribution_1_66kV and Distribution_2_11kV are also included.

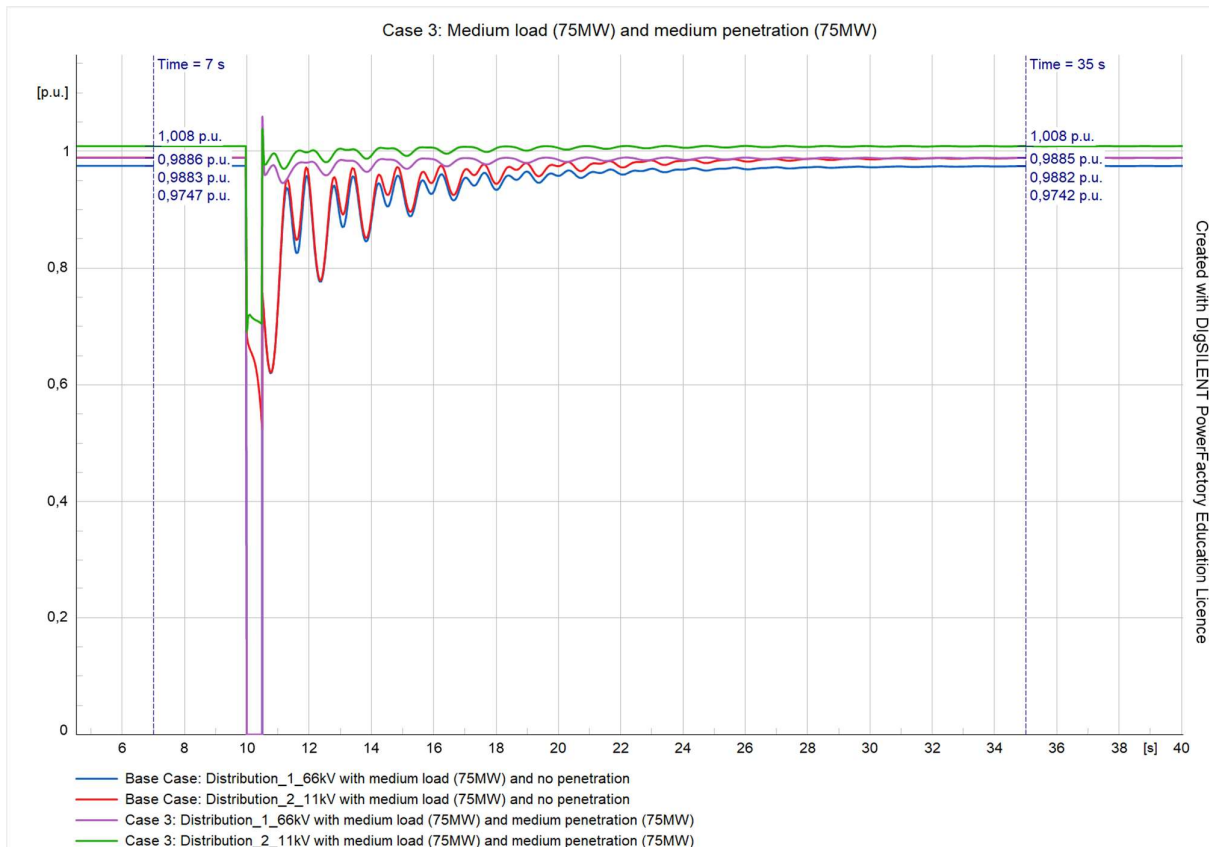


Figure 4-11: Voltage profile for Case 3 with medium penetration levels

The analysis of Figure 4-11 is as follows:

Between times $0 < t < 10$ s, the system operates normally before the occurrence of the three-phase fault.

The voltage magnitude of Distribution_1_66kV at $t=7$ s is 0.9883p.u and the voltage magnitude of Distribution_2_11kV at $t=7$ s is 1.008p.u.

The three-phase fault occurs at $t=10$ s.

Between $10 < t < 10.5$ s the system experienced oscillation as it was recovering from the three-phase fault that was created.

At $t=35$ s the system has returned to its stable state again. The voltage magnitude of Distribution_1_66kV at $t=35$ s is 0.9885p.u and the voltage magnitude of Distribution_2_11kV at $t=35$ s is 1.008p.u. These values do not match those from time $t=7$ s, as the system did not fully recover from the fault.

The voltage magnitudes from this case for both times $t=7$ s and $t=35$ s differ from those of the base case, which indicates that there is voltage deviation. Using Equation 2-8, the voltage deviation for Distribution_1_66kV at $t=7$ s was calculated to be 1.40% and at $t=35$ s it was calculated to be 1.47%.

The voltage deviation for Distribution_2_11kV at $t=7$ s was calculated to be 1.96% and at $t=35$ s it was calculated to be 2.00%.

II. Frequency Profile

Figure 4-12 depicts the frequency profiles for Distribution_1_66kV and Distribution_2_11kV where the system consisted of medium loads (75MW) and medium levels of penetration (75MW) were applied. The base case frequency profiles for Distribution_1_66kV and Distribution_2_11kV are also included.

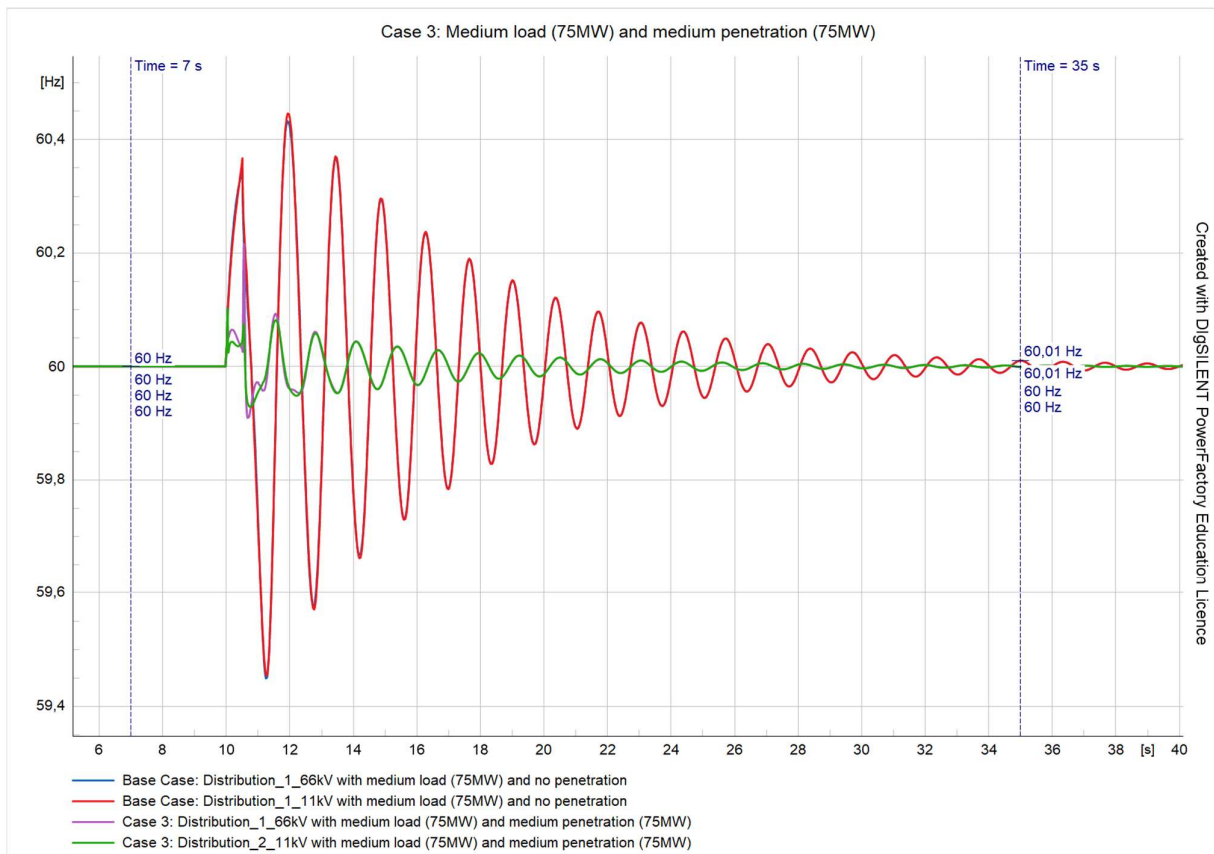


Figure 4-12: Frequency profile for Case 3 with medium penetration levels

The analysis of Figure 4-12 is as follows:

Between times $0 < t < 10$ s, the system operates normally before the occurrence of the three-phase fault.

The frequency magnitude of Distribution_1_66kV at $t=7$ s is 60Hz and the frequency magnitude of Distribution_2_11kV at $t=7$ s is 60Hz.

The three-phase fault occurs at $t=10$ s.

Between $10 < t < 10.5$ s the system experienced oscillation as it was recovering from the three-phase fault that was created.

At $t=35$ s the system has returned to its stable state again. The frequency magnitude of Distribution_1_66kV at $t=35$ s is 60Hz and the frequency magnitude of Distribution_2_11kV at $t=35$ s is 60Hz. These values do not match those from time $t=7$ s, as the system did not fully recover from the fault.

The frequency magnitudes from this case for both times $t=7$ s and $t=35$ s differ from those of the base case, which indicates that there is frequency deviation. Using Equation 2-8 the frequency deviation for Distribution_2_11kV at $t=7$ s and $t=35$ s was calculated to be 0%.

The frequency deviation for Distribution_2_11kV at $t=7$ s and $t=35$ s was calculated to be -0.02%.

4.3.3. High Penetration Levels

I. Voltage Profile

Figure 4-13 depicts the voltage profiles for Distribution_1_66kV and Distribution_2_11kV where the system consisted of medium loads (75MW) and high levels of penetration (100MW) were applied. The base case voltage profiles for Distribution_1_66kV and Distribution_2_11kV are also included.

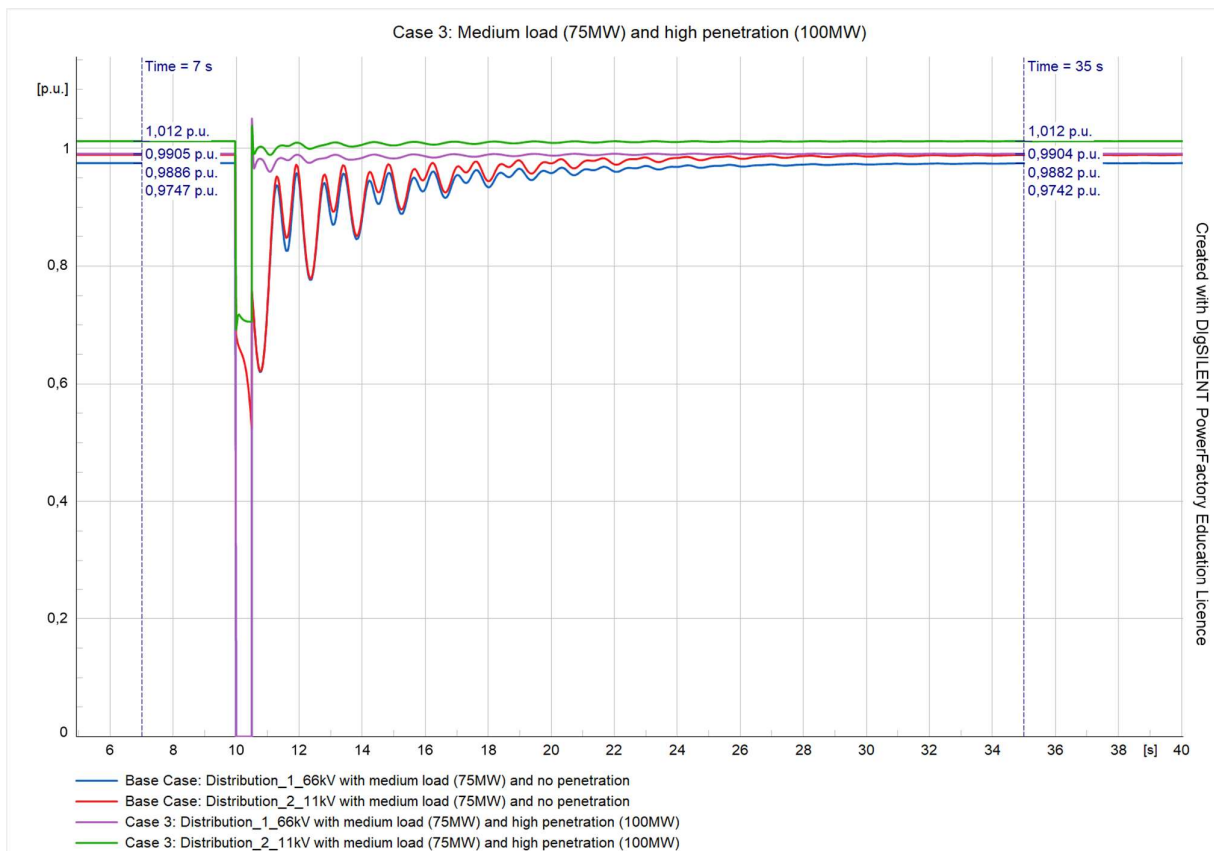


Figure 4-13: Voltage profile for Case 3 with high penetration levels

The analysis of Figure 4-13 is as follows:

Between times $0 < t < 10$ s, the system operates normally before the occurrence of the three-phase fault.

The voltage magnitude of Distribution_1_66kV at $t=7$ s is 0.9905p.u and the voltage magnitude of Distribution_2_11kV at $t=7$ s is 1.012p.u.

The three-phase fault occurs at $t=10$ s.

Between $10 < t < 10.5$ s the system experienced oscillation as it was recovering from the three-phase fault that was created.

At $t=35$ s the system has returned to its stable state again. The voltage magnitude of Distribution_1_66kV at $t=35$ s is 0.9904p.u and the voltage magnitude of Distribution_2_11kV at $t=35$ s is 1.012p.u. These values do not match those from time $t=7$ s, as the system did not fully recover from the fault.

The voltage magnitudes from this case for both times $t=7$ s and $t=35$ s differ from those of the base case, which indicates that there is voltage deviation. Using Equation 2-8, the voltage deviation for Distribution_1_66kV at $t=7$ s was calculated to be 1.62% and at $t=35$ s it was calculated to be 1.66%.

The voltage deviation for Distribution_2_11kV at $t=7$ s was calculated to be 2.37% and at $t=35$ s it was calculated to be 2.41%.

II. Frequency Profile

Figure 4-14 depicts the frequency profiles for Distribution_1_66kV and Distribution_2_11kV where the system consisted of medium loads (75MW) and high levels of penetration (100MW) were applied. The base case frequency profiles for Distribution_1_66kV and Distribution_2_11kV are also included.

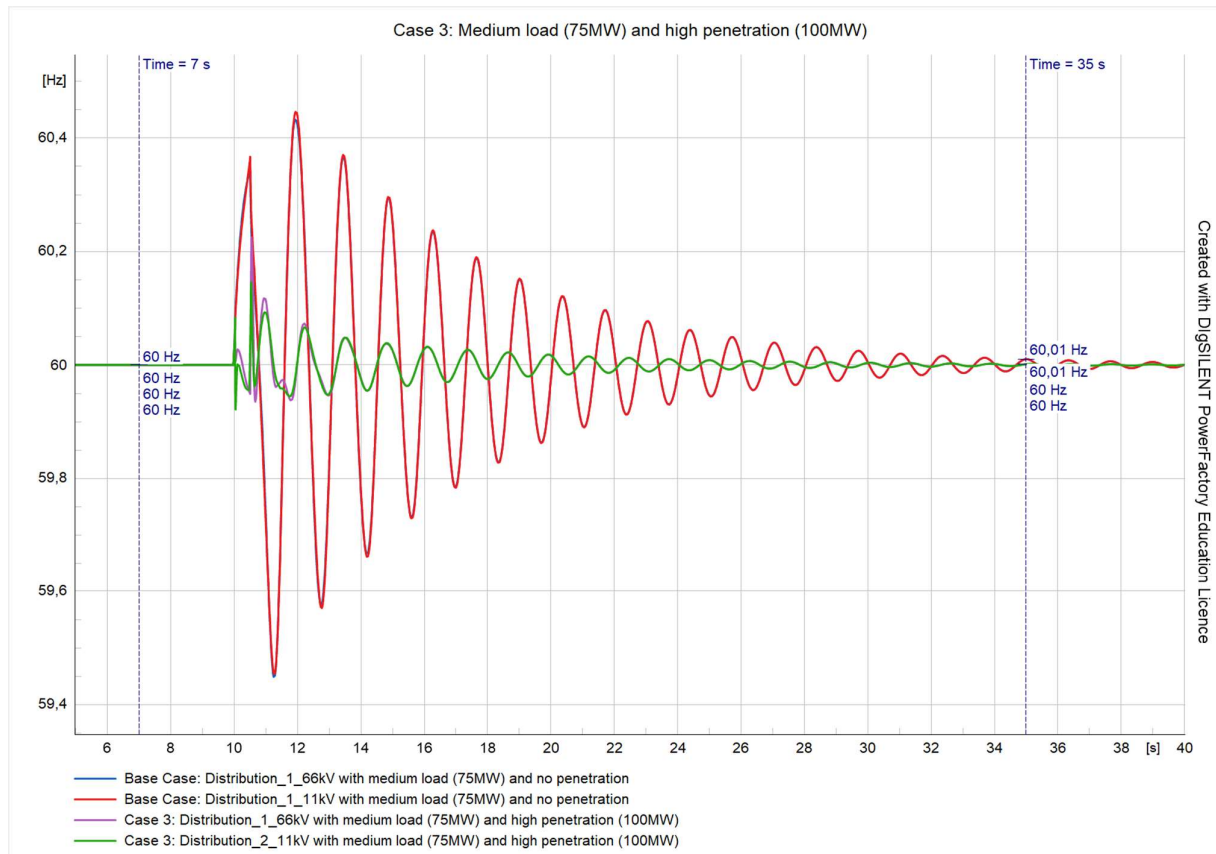


Figure 4-14: Frequency profile for Case 3 with high penetration levels

The analysis of Figure 4-14 is as follows:

Between times $0 < t < 10$ s, the system operates normally before the occurrence of the three-phase fault.

The frequency magnitude of Distribution_1_66kV at $t=7$ s is 60Hz and the frequency magnitude of Distribution_2_11kV at $t=7$ s is 60Hz.

The three-phase fault occurs at $t=10$ s.

Between $10 < t < 10.5$ s the system experienced oscillation as it was recovering from the three-phase fault that was created.

At $t=35$ s the system has returned to its stable state again. The frequency magnitude of Distribution_1_66kV at $t=35$ s is 60Hz and the frequency magnitude of Distribution_2_11kV at $t=35$ s is 60Hz. These values do not match those from time $t=7$ s, as the system did not fully recover from the fault.

The frequency magnitudes from this case for both times $t=7$ s and $t=35$ s differ from those of the base case, which indicates that there is frequency deviation. Using Equation 2-8 the frequency deviation for Distribution_2_11kV at $t=7$ s and $t=35$ s was calculated to be 0%.

The frequency deviation for Distribution_2_11kV at $t=7$ s and $t=35$ s was calculated to be -0.02%.

4.4. Case study 4: Voltage and frequency simulations of the system with high loads (100MW) and with varying levels of penetration

4.4.1. Low Penetration Levels

I. Voltage Profile

Figure 4-15 depicts the voltage profiles for Distribution_1_66kV and Distribution_2_11kV where the system consisted of high loads (100MW) and low levels of penetration (50MW) was applied. The base case voltage profiles for Distribution_1_66kV and Distribution_2_11kV are also included.

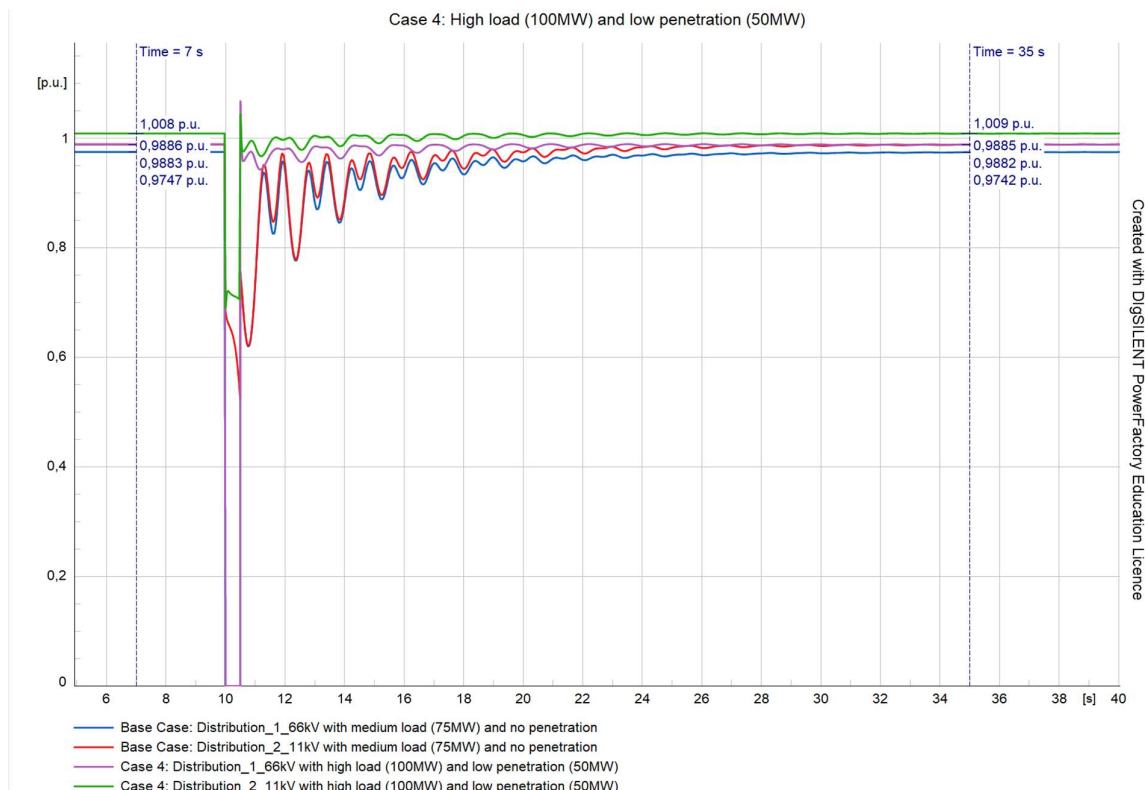


Figure 4-15: Voltage profile for Case 4 with low penetration levels

The analysis of Figure 4-15 is as follows:

Between times $0 < t < 10$ s, the system operates normally before the occurrence of the three-phase fault.

The voltage magnitude of Distribution_1_66kV at $t=7$ s is 0.9883p.u and the voltage magnitude of Distribution_2_11kV at $t=7$ s is 1.008p.u.

The three-phase fault occurs at $t=10$ s.

Between $10 < t < 10.5$ s the system experienced oscillation as it was recovering from the three-phase fault that was created.

At $t=35$ s the system has returned to its stable state again. The voltage magnitude of Distribution_1_66kV at $t=35$ s is 0.9885p.u and the voltage magnitude of Distribution_2_11kV at $t=35$ s is 1.009p.u. These values do not match those from time $t=7$ s, as the system did not fully recover from the fault.

The voltage magnitudes from this case for both times $t=7$ s and $t=35$ s differ from those of the base case, which indicates that there is voltage deviation. Using Equation 2-8, the voltage deviation for Distribution_1_66kV at $t=7$ s was calculated to be 1.40% and at $t=35$ s it was calculated to be 1.47%.

The voltage deviation for Distribution_2_11kV at $t=7$ s was calculated to be 1.96% and at $t=35$ s it was calculated to be 2.10%.

II. Frequency Profile

Figure 4-16 depicts the frequency profiles for Distribution_1_66kV and Distribution_2_11kV where the system consisted of high loads (100MW) and low levels of penetration (50MW) applied. The base case frequency profiles for Distribution_1_66kV and Distribution_2_11kV are also included.

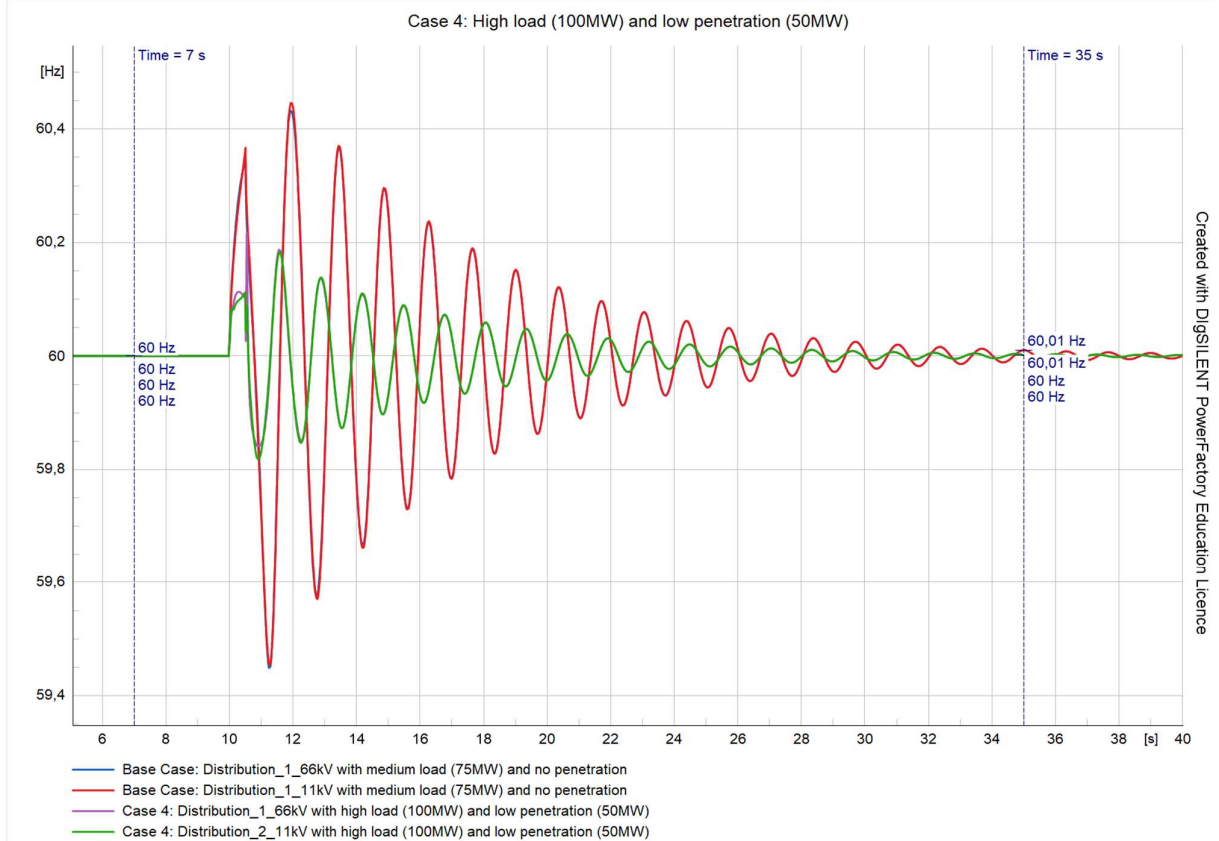


Figure 4-16: Frequency profile for Case 4 with low penetration levels

The analysis of Figure 4-16 is as follows:

Between times $0 < t < 10$ s, the system operates normally before the occurrence of the three-phase fault.

The frequency magnitude of Distribution_1_66kV at $t=7$ s is 60Hz and the frequency magnitude of Distribution_2_11kV at $t=7$ s is 60Hz.

The three-phase fault occurs at $t=10$ s.

Between $10 < t < 10.5$ s the system experienced oscillation as it was recovering from the three-phase fault that was created.

At $t=35$ s the system has returned to its stable state again. The frequency magnitude of Distribution_1_66kV at $t=35$ s is 60Hz and the frequency magnitude of Distribution_2_11kV at $t=35$ s is 60Hz. These values do not match those from time $t=7$ s, as the system did not fully recover from the fault.

The frequency magnitudes from this case for both times $t=7$ s and $t=35$ s differ from those of the base case, which indicates that there is frequency deviation. Using Equation 2-8 the frequency deviation for Distribution_2_11kV at $t=7$ s and $t=35$ s was calculated to be 0%.

The frequency deviation for Distribution_2_11kV at $t=7$ s and $t=35$ s was calculated to be -0.02%.

4.4.2. Medium Penetration Levels

I. Voltage Profile

Figure 4-17 depicts the voltage profiles for Distribution_1_66kV and Distribution_2_11kV where the system consisted of high loads (100MW) and medium levels of penetration (75MW) were applied. The base case voltage profiles for Distribution_1_66kV and Distribution_2_11kV are also included.

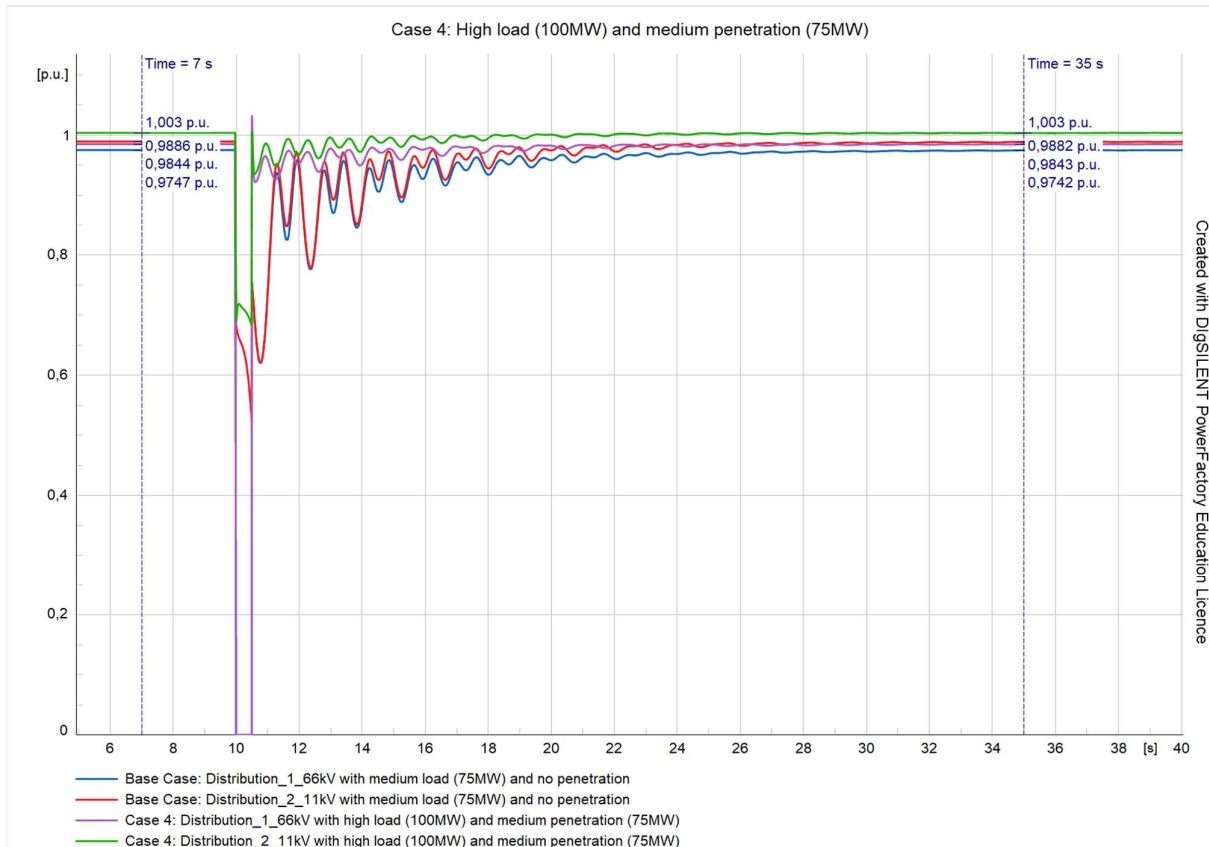


Figure 4-17: Voltage profile for Case 4 with medium penetration levels

The analysis of Figure 4-17 is as follows:

Between times $0 < t < 10$ s, the system operates normally before the occurrence of the three-phase fault.

The voltage magnitude of Distribution_1_66kV at $t=7$ s is 0.9844p.u and the voltage magnitude of Distribution_2_11kV at $t=7$ s is 1.003p.u.

The three-phase fault occurs at $t=10$ s.

Between $10 < t < 10.5$ s the system experienced oscillation as it was recovering from the three-phase fault that was created.

At $t=35$ s the system has returned to its stable state again. The voltage magnitude of Distribution_1_66kV at $t=35$ s is 0.9843p.u and the voltage magnitude of Distribution_2_11kV at $t=35$ s is 1.003p.u. These values do not match those from time $t=7$ s, as the system did not fully recover from the fault.

The voltage magnitudes from this case for both times $t=7$ s and $t=35$ s differ from those of the base case, which indicates that there is voltage deviation. Using Equation 2-8, the voltage deviation for Distribution_1_66kV at $t=7$ s was calculated to be 1.00% and at $t=35$ s it was calculated to be 1.04%.

The voltage deviation for Distribution_2_11kV at $t=7$ s was calculated to be 1.46% and at $t=35$ s it was calculated to be 1.50%.

II. Frequency Profile

Figure 4-18 depicts the frequency profiles for Distribution_1_66kV and Distribution_2_11kV where the system consisted of high loads (100MW) and medium levels of penetration (75MW) were applied. The base case frequency profiles for Distribution_1_66kV and Distribution_2_11kV are also included.

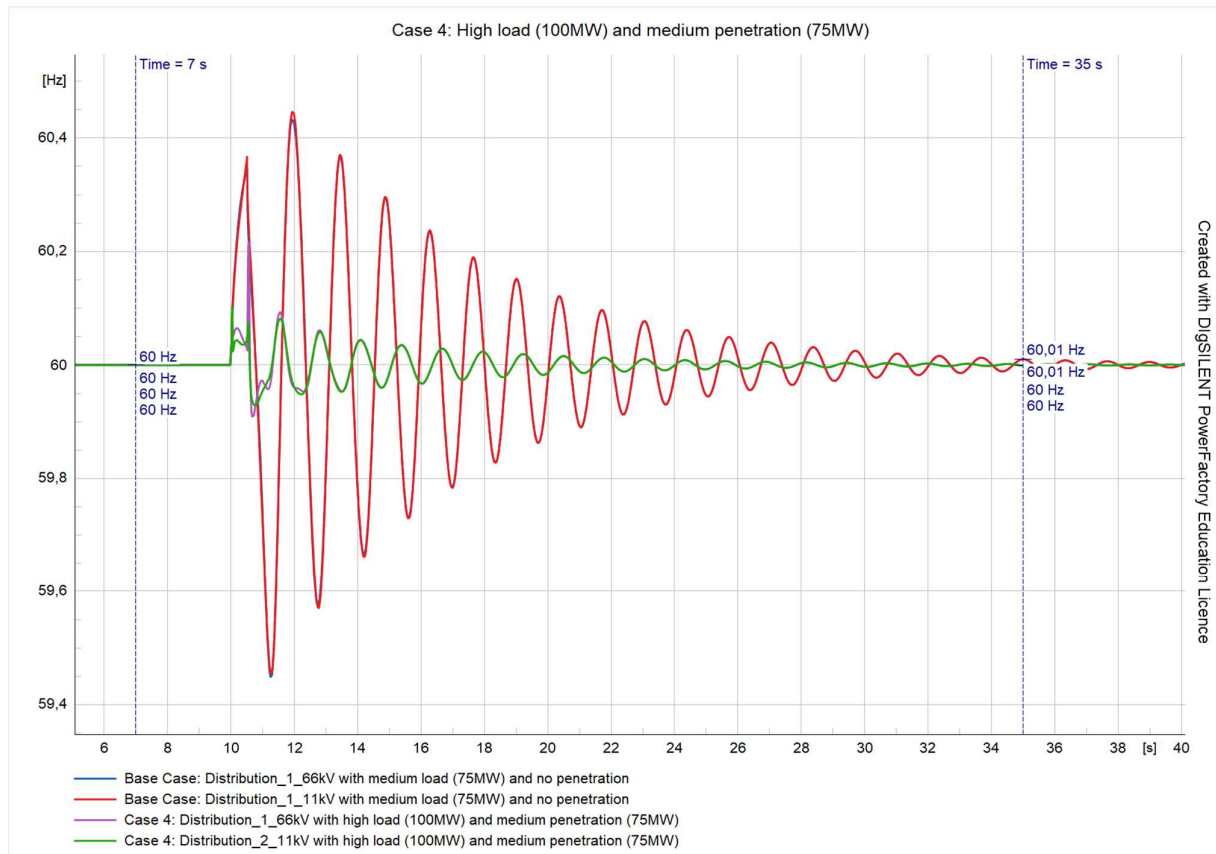


Figure 4-18: Frequency profile for Case 4 with medium penetration levels

The analysis of Figure 4-19 is as follows:

Between times $0 < t < 10$ s, the system operates normally before the occurrence of the three-phase fault.

The voltage magnitude of Distribution_1_66kV at $t=7$ s is 0.9913p.u and the voltage magnitude of Distribution_2_11kV at $t=7$ s is 1.014p.u.

The three-phase fault occurs at $t=10$ s.

Between $10 < t < 10.5$ s the system experiences oscillation as it is recovering from the three-phase fault that was created.

At $t=35$ s the system has returned to its stable state again. The voltage magnitude of Distribution_1_66kV at $t=35$ s is 0.9909p.u and the voltage magnitude of Distribution_2_11kV at $t=35$ s is 1.013p.u. These values do not match those from time $t=7$ s, as the system did not fully recover from the fault.

The voltage magnitudes from this case for both times $t=7$ s and $t=35$ s differ from those of the base case, which indicates that there is voltage deviation. Using Equation 2-8, the voltage deviation for Distribution_1_66kV at $t=7$ s was calculated to be 1.70% and at $t=35$ s it was calculated to be 1.71%.

The voltage deviation for Distribution_2_11kV at $t=7$ s was calculated to be 2.57% and at $t=35$ s it was calculated to be 2.51%.

II. Frequency Profile

Figure 4-20 depicts the voltage profiles for Distribution_1_66kV and Distribution_2_11kV where the system consisted of high loads (100MW) and high levels of penetration (100MW) were applied. The base case voltage profiles for Distribution_1_66kV and Distribution_2_11kV are also included.

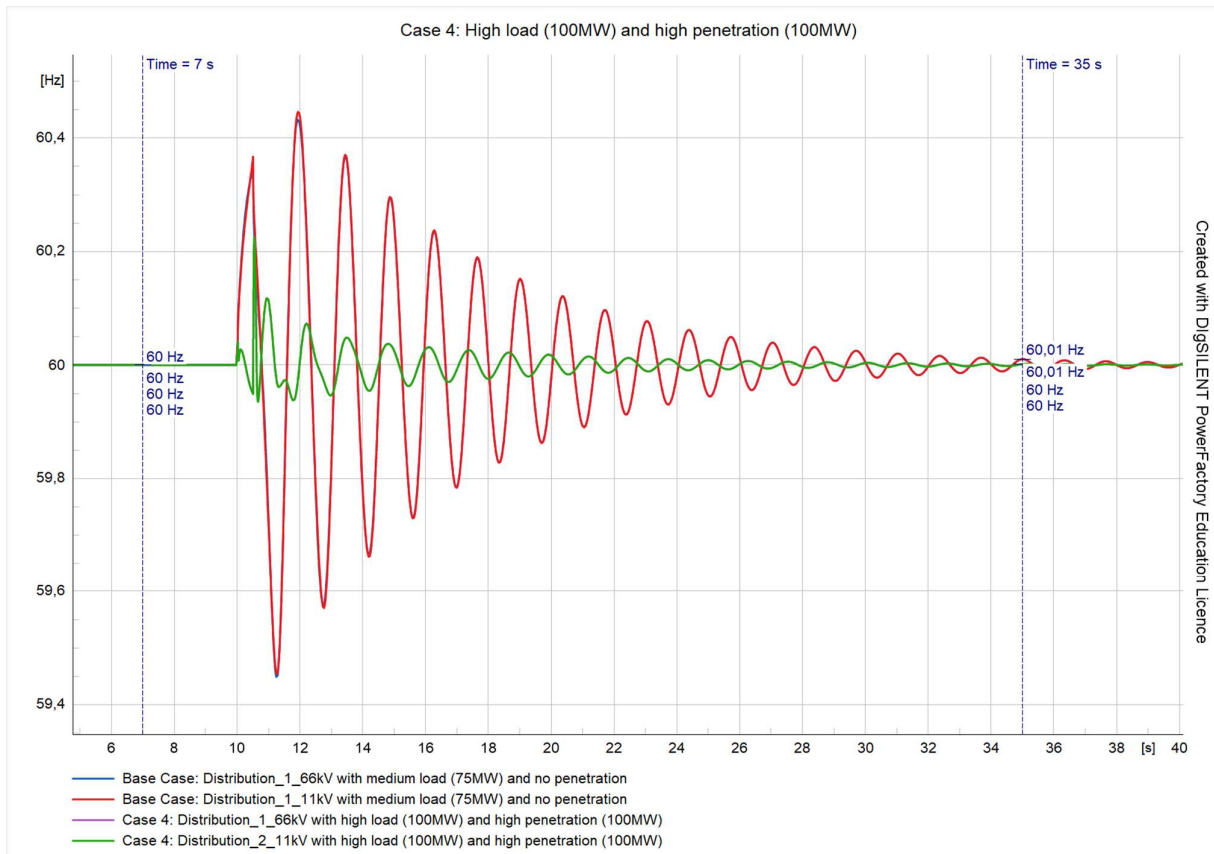


Figure 4-20: Frequency profile for Case 4 with high penetration levels

5. Conclusion

This chapter concludes the thesis by summarizing the results and outlining the limitations. Additionally, it includes recommendations for future work in this field of study.

5.1. Conclusions

In conclusion, the impact of residential solar photovoltaic system integration on power quality in a distribution network was investigated and all the objectives of the thesis were met. A review of the impact of residential solar PV system integration on power quality in a distribution network was done, which aided in the understanding of the project requirements. A test system which consisted of distribution networks and PV plant integration was built on DIgSILENT PowerFactory and voltage and frequency profiles were generated to analyse the power quality for different cases. The results showed there were significant voltage deviations in both distribution networks for all cases, however, there was very little deviation present in the frequency profiles. The results also indicate that distribution networks that operate at lower voltage levels are more likely to experience greater power quality challenges than those that operate at higher voltage levels. High penetration levels affected the voltage deviations the most, while low penetration levels affected the voltage deviations the least. The system experienced greater power quality challenges under medium loads, compared to systems consisting of the low and high loads. Lastly, the voltage levels of the distribution networks complied with the South African Grid Codes for DG integration.

Limitations of the project included time constraints, as a single academic semester was given to complete it. Load-shedding was also a limitation that affected the progress of the thesis as it occurred daily for several weeks throughout the semester.

5.2. Recommendations for Future work

The following recommendations for future work in this field of study are made to outline ways in which this project can be expanded and improved upon.

5.2.1. Consideration of Other Types of DG Systems

Other types of DG systems such as wind and hydroelectric power can be investigated to determine how they affect power quality in a residential distribution network.

5.2.2. Variation of the Grid Strength

The grid strength can be varied to determine how power quality is affected in grids of various strengths.

5.2.3. Different Short Circuit Events

Several different types of short circuit events are available on DIgSILENT that could be applied to the system instead of a three-phase fault.

5.2.4. Consideration of Multiple Points of Integration

The PV plants can be integrated at different points of the transmission system, such as buses that are closer to the synchronous generators to observe how power quality is affected under these conditions.

- [16] S. Ashfaq, "Design and Cost Evaluation of a Distribution Feeder Connected Solar System," 2014, doi: 10.0013/0027.
- [17] J. Susanto, F. Shahnia, and D. Ludwig, "A framework to technically evaluate integration of utility-scale photovoltaic plants to weak power distribution systems," *Appl Energy*, vol. 231, pp. 207-221, Dec. 2018, doi: 10.1016/j.apenergy.2018.09.130.
- [18] A. Hoke, R. Butler, J. Hambrick, and B. Kroposki, "Maximum Photovoltaic Penetration Levels on Typical Distribution Feeders Preprint Maximum Photovoltaic Penetration Levels on Typical Distribution Feeders," 2012. [Online]. Available: <http://www.osti.gov/bridge>
- [19] Q. Sun *et al.*, "Three-dimensional modeling on lightning induced overvoltage for photovoltaic arrays installed on mountain," *J Clean Prod*, vol. 288, Mar. 2021, doi: 10.1016/j.jclepro.2020.125084.
- [20] R. Sangeepu and V. Muni, "Effect of Power Quality Issues in Power System and Its Mitigation by Power Electronics Devices," 2015. [Online]. Available: www.discovery.org.in/www.discovery.org.in/d.htm
- [21] IEEE Power & Energy Society, IEEE Industry Applications Society, and Institute of Electrical and Electronics Engineers, *2019 IEEE PES International Conference on Innovative Smart Grid Technologies Asia (ISGT 2019) : May 21-24, 2019, Chengdu, China*.
- [22] K. Rahimi, S. Mohajeryami, and A. Majzoobi, "Effects of photovoltaic systems on power quality," in *NAPS 2016 - 48th North American Power Symposium, Proceedings*, Nov. 2016. doi: 10.1109/NAPS.2016.7747955.
- [23] L. Collins and J. K. Ward, "Real and reactive power control of distributed PV inverters for overvoltage prevention and increased renewable generation hosting capacity," *Renew Energy*, vol. 81, pp. 464-471, Sep. 2015, doi: 10.1016/j.renene.2015.03.012.
- [24] N. B. G. (Nico) Brinkel *et al.*, "Impact of rapid PV fluctuations on power quality in the low-voltage grid and mitigation strategies using electric vehicles," *International Journal of Electrical Power and Energy Systems*, vol. 118, Jun. 2020, doi: 10.1016/j.ijepes.2019.105741.
- [25] S. Shivashankar, S. Mekhilef, H. Mokhlis, and M. Karimi, "Mitigating methods of power fluctuation of photovoltaic (PV) sources - A review," *Renewable and Sustainable Energy Reviews*, vol. 59. Elsevier Ltd, pp. 1170-1184, Jun. 01, 2016. doi: 10.1016/j.rser.2016.01.059.
- [26] K. Abo-Al-Ez, E. A. Badran, H. Muaelou, K. M. Abo-Al-Ez, and E. A. Badran, "Control Design of Grid-Connected PV Systems for Power Factor Correction in Distribution Power Systems Using PSCAD High Impedance Fault Detection View project Special Issue 'Optimization and Control in Energy Management'-MATHEMATICS, MDPI View project Control Design of Grid-Connected PV Systems for Power Factor Correction in Distribution Power Systems Using PSCAD," *Article in International Journal of Scientific and Engineering Research*, vol. 6, no. 8, 2015, [Online]. Available: <http://www.ijser.org>
- [27] Q. Liu, Y. Li, L. Luo, Y. Peng, and Y. Cao, "Power Quality Management of PV Power Plant With Transformer Integrated Filtering Method," *IEEE Transactions on Power Delivery*, vol. 34, no. 3, pp. 941-949, Jun. 2019, doi: 10.1109/TPWRD.2018.2881991.
- [28] L. Alhafadhi, C. M. Lai, J. Teh, and M. Salem, "Predictive adaptive filter for reducing total harmonics distortion in PV systems," *Energies (Basel)*, vol. 13, no. 12, Jun. 2020, doi: 10.3390/en13123286.
- [29] H. M. Sultan, A. A. Zaki Diab, O. N. Kuznetsov, Z. M. Ali, and O. Abdalla, "Evaluation of the impact of high penetration levels of PV power plants on the capacity, frequency and voltage stability of Egypt's unified grid," *Energies (Basel)*, vol. 12, no. 3, Feb. 2019, doi: 10.3390/en12030552.
- [30] "PSCAD TM IEEE 09 Bus System," 2018.
- [31] M. C. Shekar and N. Aarthi, "Contingency Analysis of IEEE 9 Bus System," in *2018 3rd IEEE International Conference on Recent Trends in Electronics, Information and Communication Technology, RTEICT 2018 - Proceedings*, May 2018, pp. 2225-2229. doi: 10.1109/RTEICT42901.2018.9012467.

- [32] D. Powerfactory, "Nine-bus System." [Online]. Available: www.digsilent.de
- [33] B. ÇAVDAR, Ö. AKYAZI, E. SAHIN, and F. NUROGLU, "Voltage Stability Analysis of Large Scale PV Plant Reactive Power Control Methods," *Sakarya University Journal of Science*, Jun. 2021, doi: 10.16984/saufenbilder.808343.
- [34] Mass.) IEEE Power & Energy Society. General Meeting (2016 : Boston and Institute of Electrical and Electronics Engineers., *2016 IEEE Power and Energy Society General Meeting (PESGM) : date, 17-21 July 2016*.
- [35] "Technical Reference WECC Photovoltaic Templates WECC Dist. Small PV Plants 25MVA, WECC Large-scale PV Plant 110MVA," 2022. [Online]. Available: <https://www.digsilent.de>
- [36] A. S. Saidi, M. E. Mudwah, and K. ben Kilani, "Assessment of PV systems stability under temperature variation," in *2018 9th International Renewable Energy Congress, IREC 2018*, May 2018, pp. 1–6. doi: 10.1109/IREC.2018.8362536.
- [37] Nevşehir Hacı Bektaş Veli Üniversitesi, Institute of Electrical and Electronics Engineers, Institute of Electrical and Electronics Engineers. Region 8, and Institute of Electrical and Electronics Engineers. Turkey Section, *2019 IEEE 1st Global Power, Energy and Communication Conference (GPECOM2019) : proceedings : Perissia Hotel & Convention Center, Nevşehir, Turkey, 12-15 June, 2019*.
- [38] J. M. Pearce, "Expanding photovoltaic penetration with residential distributed generation from hybrid solar photovoltaic and combined heat and power systems," *Energy*, vol. 34, no. 11, pp. 1947–1954, 2009, doi: 10.1016/j.energy.2009.08.012.
- [39] S. I. Ao and International Association of Engineers., *World Congress on Engineering and Computer Science : WCECS 2012 : 24-26 October, 2012, San Francisco, USA*. Newswood Ltd., International Association of Engineers, 2012.
- [40] M. Ghazavi Dozein, P. Mancarella, T. Kumar Saha, and R. Yan, "System Strength and Weak Grids: Fundamentals, Challenges, and Mitigation Strategies; System Strength and Weak Grids: Fundamentals, Challenges, and Mitigation Strategies," 2018.

Appendices

Appendix A: System Report and Penetration Levels Percentage Calculations

		DIGSILENT PowerFactory 2022 SP2	Project: - Date: 2022/11/04				
Load Flow Calculation	Complete System Report: Voltage Profiles, Grid Interchange						
AC Load Flow, balanced, positive sequence Automatic tap adjustment of transformers Consider reactive power limits	No No	Automatic Model Adaptation for Convergence Max. Acceptable Load Flow Error Bus Equations(HV) Model Equations	No 1,00 kVA 0,10 %				
Total System Summary	Study Case: Base Case Volt						
Generation [MW]/ [Mvar]	Motor Load [MW]/ [Mvar]	Compens- sation [MW]/ [Mvar]	External Infeed [MW]/ [Mvar]	Inter Area Flow [MW]/ [Mvar]	Total Losses [MW]/ [Mvar]	Load Losses [MW]/ [Mvar]	No load Losses [MW]/ [Mvar]
\Crystal Jaftha\Nine-bus System(1)\Network Model\Network Data\Nine-bus System				0,00	7,83	7,83	0,00
472,83	0,00	465,00	0,00	0,00	-39,34	96,99	-136,33
89,83	0,00	115,00	0,00	-14,16			
Total:	472,83	0,00	465,00	0,00	7,83	7,83	0,00
	89,83	0,00	115,00	0,00	-39,34	96,99	-136,33

Figure A-1: Complete system report

Penetration Levels Percentage Calculations:

$$\begin{aligned}
 \text{Low Penetration Level \%} &= \frac{\text{Active Power}}{\text{Total Load}} \times 100 \\
 &= \frac{50\text{MW}}{465\text{MW}} \times 100 \\
 &= 11\%
 \end{aligned}$$

$$\begin{aligned}
 \text{Medium Penetration Level \%} &= \frac{\text{Active Power}}{\text{Total Load}} \times 100 \\
 &= \frac{75\text{MW}}{465\text{MW}} \times 100 \\
 &= 16\%
 \end{aligned}$$

$$\begin{aligned}
 \text{High Penetration Level \%} &= \frac{\text{Active Power}}{\text{Total Load}} \times 100 \\
 &= \frac{100\text{MW}}{465\text{MW}} \times 100 \\
 &= 22\%
 \end{aligned}$$

